

**USMANU DANFODIYO UNIVERSITY, SOKOTO
(POSTGRADUATE SCHOOL)**

**CATALYTIC CONVERSION OF HEMICELLULOSE OBTAINED FROM
MAIZE COBS TO LIQUID HYDROCARBONS**

**A Dissertation
Submitted to the
Postgraduate School,
USMANU DANFODIYO UNIVERSITY, SOKOTO, NIGERIA**

**In Partial Fulfillment of the Requirements
For the Award of the Degree of
MASTER OF SCIENCE (PETROLEUM CHEMISTRY)**

BY

MUHAMMAD, Gambo

(ADM. NO. 16210313005)

DEPARTMENT OF PURE AND APPLIED CHEMISTRY

OCTOBER, 2019

DEDICATION

This work is dedicated to my beloved parents, Mallam Muhammad Bulu and Mallama Hauwa Muhammad.

CERTIFICATION

This Dissertation by MUHAMMAD GAMBO (ADM. NO. 16210313005) has met the requirements for the award of the Degree of Master of Science (Petroleum Chemistry) of the Usmanu Danfodiyo University, Sokoto and is approved for its contribution to the knowledge.

(External Examiner)

Date

Dr. M.N. Almustapha

Date

(Major Supervisor)

Dr. M.G. Liman

Date

(Co- Supervisor I)

Dr. A.B. Rabah

Date

(Co- Supervisor II)

Prof. A.B. Mohammed

Date

(Head of Department)

ACKNOWLEDGEMENTS

All praise and adoration goesto Allah the lord of the worlds, the Beneficent the omniscient and omnipotent. I'm grateful toAllah for the blessings of life, health and for sparing my soul to witness the beginning and the end of this work. This indeed wasn't by my shrewdness or specialty, rather by His blessings and power. The infinite peace be upon the first and last messenger of Allah, Muhammad (S.A.W)

I would like to convey my gratefulness to the great people behind the success of this work. First and foremost, to my supervisory team Dr. M.N. Almustapha (Major supervisor), Dr. M.G. Liman (Co-supervisor I) and Dr. A.B. Rabah (Co-supervisor II) for their understanding, guidance, courage and passion to make this work possible. I will forever be grateful.

I would like to acknowledge the valuable input from my respectful lecturers in persons of Prof. U.A. Birnin-Yauri, Prof. A.B. Muhammad, Prof. L.G. Hassan, Prof. B.U. Bagudo, Prof. U.Z. Faruq, Prof. A.I. Tsafe, Prof. S.M. Dangoggo, Dr. A.M. Sokoto, Dr. M.U. Dabai, Dr. M.L. Muhammad, Mal. A.S. Yelwa, Mal. J. Sani and entire staff members of the Department of Pure and Applied Chemistry for their insightful comments and supports throughout the program.

I would like to express my utmost gratitude to my parents for their love, prayer, sponsorship, guidance and supports, may almighty Allah grant them the highest rank in Jannah. My profound greetings go to my siblings in persons of Abdulkadir Muhammad, Malah Ali, Sulaiman Muhammad, Aisha Ali, Yagana Muhammad and Bala Muhammad, I say a big thank you for all you've done to me throughout the course of my program.

Finally, yet importantly, my deep appreciation goes to all my friends at home, your support will never be forgotten. I also want to acknowledged the help, effort and enthusiasm of Muhammad Sabi'u Jibrin and my course mates Mustapha Lawan Kar, Umar Abba Aji, Muhammad Yahaya, Shu'aibu Hassan Jatau, Sunusi Muhammad Sambo, Hamisu Ibrahim, Muhammad Adamu and all class of 2015/2016 P.G students of Pure and Applied Chemistry Department for their amazing friendship we shared during our stay. May Almighty Allah, in his boundless mercy, unite us all in the best paradise in Heaven amen.

TABLE OF CONTENTS

TITLE PAGE	i
DEDICATION	ii
CERTIFICATION	iii
ACKNOWLEDGEMENTS	iv
TABLE OF CONTENTS	vi
LIST OF PLATES	ix
LIST OF FIGURES	x
LIST OF TABLES	xi
ABBREVIATIONS	xii
ABSTRACT	xiii
CHAPTER ONE	1
1.1 INTRODUCTION	1
1.1.1 Botanical description of maize	4
1.2 Literature Review	7
1.2.1 Aqueous phase processing of biomass	7
1.2.2 Basic contents of biomass	8
1.2.3 The production of furfural and conversion process	10
1.2.4 Aldol Condensation	12
1.2.5 Hydrotreating of bio-oil	14
1.2.6 Statement of the problem	15
1.2.7 Justification of the study	16
1.2.8 Aim and objectives	17
1.2.9 Scope and delimitation	17

CHAPTER TWO18

MATERIALS AND METHODS18

2.1 Materials18

2.1.1 Sample collection 19

2.2. Methods20

2.2.1 Preparation of reagents20

2.2.2 Catalyst preparations21

2.2.3 Experiment *design* 21

2.2.4 Effect of variables21

2.2.5 Production of furfural23

2.2.6 Aldol condensation24

2.2.7 Hydrodeoxygenation25

CHAPTER THREE28

RESULTS AND DISCUSSION28

3.1 Results28

3.2 Effect ofProcess Variables32

3.3 Identifcation of Furfural35

3.4 Analysis of Aldol Adduct36

3.5 Catalyst Characterization37

3.6Analysis of Hydrodeoxygenation Products 39

CHAPTER FOUR41

CONCLUSION AND RECOMMENDATIONS41

4.1 Conclusion41

4.2 Recommendations41

References42

Appendices58

LIST OF PLATES

Plate		Page
1.1	Maize Seeds	5
1.2	Maize Cobs Used in the Research	6
2.1	Setup of Furfural Production	23
2.2	Setup Showing Condensation of Furfural with Acetone	24
2.3	Setup of Hydrodeoxygenation Process	25

LIST OF FIGURES

Figure		Page
1.1	The Main Lignocellulosic Biomass Composition	9
1.2	Chemical Transformation of Biomass to Liquid Hydrocarbons	11
1.3	Stepwise Reaction for Aldol Condensation of Furfural with acetone	14
3.4	Effect of Variables on Furfural Yield	30
3.5	Effect of Temperature Against Acid Concentration on Furfural Yield	33
3.6	Effect of Temperature Against Time on Furfural Yield	34
3.7	Effect of Time Against Acid Concentration on Furfural Yield	34

LIST OF TABLES

Table		Page
1.1	Scientific Classification of Maize	4
1.2	Chemical Composition of Some Biomass Resources	10
2.1	List of Chemicals Used in the Research	18
2.2	List of Instruments Used in the Research	18
2.3	Furfural Factors and Their Levels	21
2.4	Design of Experiment (Taguchi Orthogonal Array Design)	22
3.1	Effects of Variables for Furfural Production and Yield Obtained	30
3.2	Analysis of Variance (ANOVA) for Furfural Production	31
3.3	Model Summary	32
3.4	FT-IR Spectral Analysis of the Produced and Standard Furfural	35
3.5	FT-IR Spectral Analysis of the Aldol Adduct	37
3.6	The Crystallographic Parameters of NiO and Al ₂ O ₃	39
3.7	Composition of Hydrodeoxygenated Product	

ABBREVIATIONS

FAME	Fatty acid methyl ester
FT-IR	Fourier transform infra-red spectroscopy
GC-MS	Gas chromatography/ Mass spectroscopy
GHGs	Green-house gases
GPR	General purpose reagent
HDO	Hydrodeoxygenation
HMF	Hydro methyl furan
MSW	Municipal solid waste
MTHF	2-methyl tetrahydrofuran
RT	Retention time
TIC	Total ion count
XRD	X-ray diffraction
ZSM	Zeolite Socony mobil

ABSTRACT

Hemicellulose is one of the major components of non-food lignocellulosic biomass, which can be transformed into liquid hydrocarbons. In this study, Maize cobs were transformed into liquid hydrocarbons *via* acid-catalyzed hydrolysis. The transformation process involved, production of Furfural from maize cobs using acid-catalyzed hydrolysis and dehydration process, aldol condensation of the produced Furfural with acetone and hydrodeoxygenation of the aldol adduct to liquid hydrocarbons which was catalyzed by NiO/Al₂O₃. Taguchi design was used to determine the effect of variables on Furfural yield. The yield of the Furfural was found to be 72.0% at 180°C, 50 minute reaction time and 10% acid concentration. The Furfural produced was condensed with acetone to obtain furfural-acetone-furfural dimers which was subsequently subjected to hydrodeoxygenation to produce liquid hydrocarbons. GC-MS analysis revealed the presence of alkanes within the range of (C₇-C₁₅), with the selectivity of 61.08% on NiO/Al₂O₃ catalyst at the reaction temperature of 220°C, 30 bars pressure and reaction time of 1 h with heptane and decane being the major products each accounting for 28.06% and 17.65% respectively. The result revealed that hemicellulose obtained from Maize cobs could be a potential substrate for the production of liquid hydrocarbons with NiO/Al₂O₃ as hydrodeoxygenation catalyst.

CHAPTER ONE

INTRODUCTION AND LITERATURE REVIEW

1.1 Introduction

Frequent crisis in petroleum supply products leading to the possibility of its scarcity, prices instability and negative effects on the environment, led so much interest in alternative energy sources which has increased year after year (Santos *et al.*, 2013). The interest in renewable sources of energy arises because they are considered to be sustainable, hazard-free, safe and environmentally friendly (Tushar, 2010). However, the dominant resource for energy production currently is fossil fuel compared with the very low usage of renewable energy sources. Figure 1 shows the contribution of fossil fuels and renewable sources in the energy portfolio. The world total consumptions of fossil fuels, namely, oil, natural gas, and coal account for 30%, 22% and 28%, respectively for a total of 80% whereas the consumption of renewable sources accounts only for 17% (Kumar, 2010).

Fuels with small amounts of admixed biofuel (up to 5 vol. %; E5 Europe) are permitted in common gasoline or diesel engines and can be used in common vehicles without any form of adaptation. Also, fuels with higher levels of biofuel (more than 5 vol. %) are currently available in Brazil (gasoline, up to 25 % ethanol, E25), USA (10 % ethanol/90 % gasoline, E10), and Sweden (85 % ethanol/15 % gasoline, E85). Diesel containing 5–30 vol. %, example, FAME (B5, B10, and B30) are common, as

is E95 for diesel engines. However, vehicles using this type of fuel must be adapted (Soni *et al.*, 2008)

Biobutanol may be a more suitable gasoline-range biofuel than bioethanol, as it has the same energy density as bioethanol, but would increase the octane number in the gasoline pool. In addition, biobutanol has a lower vapor pressure and a lower water solubility, which simplifies handling procedures and the infrastructure.

According to Brunner (2009), biomass can be used as a raw material to produce useful chemicals as well as for producing energy. It is also known that biomass is a safe source of energy and can be used to decrease the emissions of hazardous gases such as SO_x and NO_x as well as GHGs (Pastircakova, 2004).

The concern over dwindling fossil fuels reserves with serious challenges it posed to the environment and the growing trend in energy consumption over the past decade was one of the driving forces for the researchers and industries to quest for an alternative source of liquid fuels and chemicals from renewable sources (Choudhary *et al.*, 2012).

The current energy utilization was derived almost exclusively from crude oil (95%) and depletion of these finite fossil fuel resources seems to be unavoidable in the future since these resources are exhausted faster than its regenerated. According to Mehdi *et al.* (2008) the proven reserves for oil, natural gas, and coal fuels have lifetimes of approximately 46, 59, and 118 years, respectively, at current usage rates. In particular,

crude oil is a resource with the shortest expected lifetime, and it is the predominant source of fuel for the transportation sector, which is one of the largest and fastest-growing global energy consumption sectors.

Additionally, the consumption of fossil fuels leads to emission of CO₂, causing detrimental effects on the environment that may accelerate rates of global warming.

(Xiu and Shabhasi 2012). One of the main concerns in the large-scale production of biofuels and chemicals is the consumption of edible biomass such as corn, sugarcane, soybeans, and vegetables as feedstocks for biofuels generation (Hongjun *et al.*, 2017).

This issue has motivated researchers around the world to develop second-generation technologies for processing non-edible biomass (lignocellulosic biomass) for sustainable production of new generation fuels and chemicals with zero effect to the food basket. In this respect, lignocellulosic biomass is attractive since it is abundant (Roman-Leshkov and Dumesic, 2009) and can be grown faster and more economically than food crops. Lignocellulosic biomass consists of three major components: cellulose (40-50%), hemicellulose (25-35%) and lignin (15-20%) (Gurbuz *et al.*, 2011).

Production of liquid fuels *via* aqueous-phase processing could be a promising option for harnessing biomass for fuels generation. The process is viable as it uses water-soluble feedstock at moderate temperatures and pressures (Demirbas, 2006).

Operation at such process conditions enables the processing of low-value biomass

into high-value products. The aqueous phase processing of biomass consists of four steps including hydrolysis, dehydration, aldol-condensation and hydrogenation (Huber *et al.*, 2005). In the first reaction step, biomass was converted to glucose and fructose molecules via the hydrolysis process. Then, glucose and fructose molecules were converted to hydroxyl-methyl furfural (HMF) and furfural over acid catalyst by the dehydration process (Bond *et al.*, 2010). Finally, intermediates were converted to liquid alkanes by aldol-condensation and hydrogenation over bifunctional catalyst.

1.1.1 Botanical description of maize (*Zee Mays*)

Maize (*Zea mays*) is a plant belonging to the family of grasses (*Poaceae*). It is cultivated globally and is one of the most important cereal crops worldwide. Maize is not only an important food crop for human consumption but also a basic element of animal feed and raw material for the manufacturing of many industrial products (Oladejo and Adetunji, 2012). The products include corn starch, maltodextrins, corn oil, corn syrup, and products of fermentation and distilleries. It is also being recently used in the production of biofuel (Zahra, 2012). Its scientific classification is shown in Table 1.

Table 1.1: Scientific Classification of Maize

S/N	Classifications	Scientific names
1	Kingdom	Plantae
2	Division	Magnoliophyta
3	Class	Liliopsida

4	Order	Poales
5	Family	Poaceae
6	Tribe	Maydaee
7	Genus	Zea
8	Species	Mays

Iken and Amusa, (2004).



Plate 1.1: Maize seeds. Iken and Amusa, (2004)

Plate 1.1 shows maize seeds and how is wide cultivated throughout the world and a greater weight of maize is produced each year than any other grain (Linda, 2013). Maize is a versatile crop grown over a range of agro-climatic zones. In fact, the suitability of maize to diverse environments is unmatched by any other crop. It is grown from 58°N to 40°S, from below sea level to altitudes higher than 3000 m, and in areas with 250 mm to more than 5000 mm of rainfall per year (Shaw, 1988). And with a growing cycle ranging from 3 to 13 months.



Plate 1.2: Maize cobs Used in the Research

Plate 1.2 shows threshed cobs from the grains which has methane potential and could be used as a sustainable feedstock for anaerobic digestion processes (Massimo *et al.*, 2016). Biomass is a renewable resource of carbon produced from organic matter including agricultural residues. These materials can be converted to energy carrier and/or heat as well as liquid fuels by either thermochemical, physicochemical, or biological processes

1.2 Literature Review

The use of furans, such as HMF and furfural, as precursors of liquid hydrocarbon fuels, is an option for the production of linear alkanes in the molecular weight range appropriate for gasoline to diesel or jet fuel (C₇-C₁₅) (Sokoto *et al.*, 2017). Polysaccharides can be hydrolyzed to their constituent monomers, which can subsequently be dehydrated over an acid catalyst to furan compounds with a carbonyl group such as HMF, 5-methylfurfural, or 2-furaldehyde (furfural) (Barret *et al.*, 2006).

1.2.1 Aqueous phase processing of biomass

Aldol condensation has been typically performed in the presence of base catalysts, such as NaOH (Fakhfakh *et al.*, 2008), KOH and NH₃·H₂O (Liu *et al.*, 2008). These homogeneous catalysts have been effective in decreasing reaction temperature and shortening the reaction time; however, it is difficult to separate them from the reaction solution and reuse them without causing environmental issues. Therefore, many researchers have focused on solid base catalysts in recent years (Hideshi, 2004).

In a subsequent study, West *et al.* (2008) conducted the condensation of furfural and HMF with acetone in an aqueous phase, using NaOH as a catalyst and the limited solubility of furfural in water made it necessary to use high amounts of a base to observe the substantial activity.

The use of Cu based catalysts exhibit a remarkable selectivity toward hydrogenation of the carbonyl group leaving the C=C double bonds in the furyl ring unreacted. Copper containing catalysts, such as Cu–Zn mixed oxides with Al, Mn and Fe, Cu/MgO, Cu–Ca/SiO₂ and Pt on different supports are most frequently employed for furfural hydrogenation (Merlo *et al.*, 2009).

Huber *et al.* (2005), proposed a process for obtaining diesel fuels of high quality from the condensation of HMF or furfural with acetone involving the aldol condensation, followed by hydrogenation and deep hydrodeoxygenation.

1.2.2 Basic contents of biomass

In general, biomass consists of cellulose, hemicellulose, and lignin. Fig. 1.2 shows the percentages of the basic contents of biomass (Kumar, 2010). Cellulose mainly consists of anhydrous glucose in a chain structure. The molecules of anhydroglucose are linked by β - glycosidic in a chain of linear structure, which increases the stability of cellulose. The importance of cellulose is to provide the solidity of the plant. The second major component in plants is hemicellulose, which consists of side chains of different sugars in a polymer structure. According to Bobleter (1994), these sugars could be classified either as five carbons (arabinose, and xylose) or six carbons (glucose, mannose, galactose). The hemicellulose works like glue for the cellulose units through hydrogen bonds.

The third major component in plants is lignin, which is one of the complex components present in the plants. Lignin consists mainly of different units of phenyl propane as sinapyl alcohol, p- cocumaryl alcohol, and coniferyl alcohol. Lignin works as a linkage for the plant cellular and as a protector against chemical or microorganism effects. In addition, lignin is the controller of the fluid flow through plants and it can work as an antioxidant because it absorbs UV lights (Falkehag, 1975: Olsson, *et al.*, 2005).

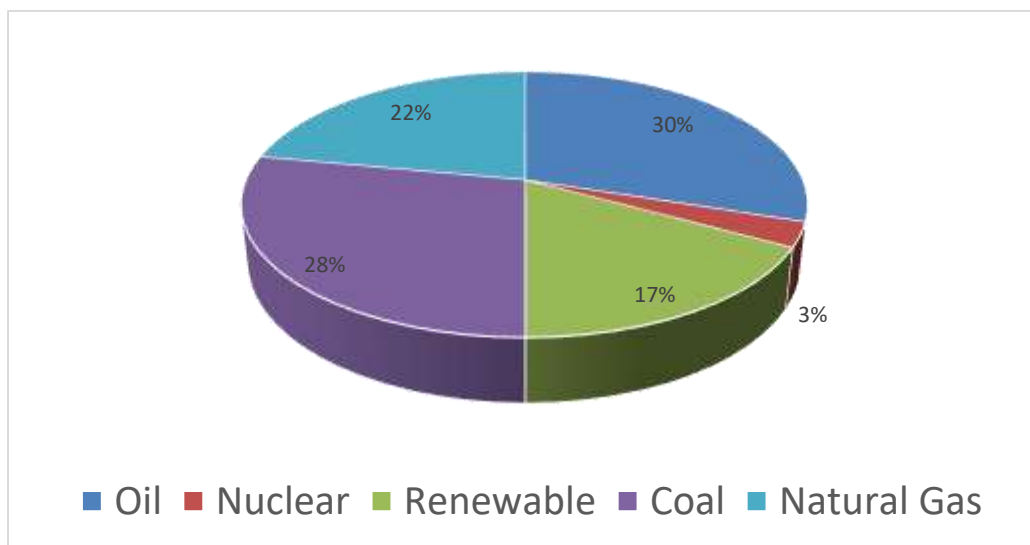


Figure 1.1: The Main Lignocellulosic Biomass Composition (Kumar, 2010)

The biomass that could be used for biofuels production will depend on regional issues such as soil quality, precipitation, and climate. Biomass can be produced not only on agricultural land but also on the forest, aquatic, and arid land (Kaygusuz *et al.*, 2015). Nature produces a wide range of structures from biomass. Plants use solar energy to combine carbon dioxide and water forming a sugar building block and oxygen. The

sugar is stored in a polymer form as cellulose, starch, or hemicellulose. Most biomass approximately contained 75 wt % sugar polymers (Huber *et al.*, 2006). The first step for biofuels production is obtaining an inexpensive and abundant biomass feedstock. Biofuel feedstocks can be chosen from the following; waste materials (agricultural wastes, crop residues, wood wastes, urban wastes), forest products (wood, logging residues, trees, shrubs), energy crops (starch crops such as corn, wheat, barley; sugar crops; grasses; woody crops; vegetable oils; hydrocarbon plants), or aquatic biomass (algae, waterweed, water hyacinth) (Kaygusuz *et al.*, 2015). The structured portion of biomass is composed of cellulose (35-50%), hemicelluloses (20-35%), lignin (15-25%) and a number of other compounds (Wyman *et al.*, 2005). The lignocellulosic composition of some locally available biomass is listed in Table 1.2

Table 1.2: Chemical Composition of Some Biomass Resources

Biomass	Cellulose (%)	Hemicellulose (%)	Lignin (%)
Finger millet hulls	25 ± 0.73	32 ± 1.38	4 ± 1.66
Sorghum hulls	39 ± 0.82	35 ± 0.07	4 ± 0.11
Corn stalk	30 ± 1.19	33 ± 2.63	15 ± 0.67
Cassava peels	39 ± 0.34	25 ± 0.41	8 ± 0.52
Saw dust	44 ± 1.77	17 ± 0.14	21 ± 1.92
Rice straw	35 ± 1.31	27 ± 1.97	16 ± 2.01

Soybean hulls	35 ± 0.12	16 ± 0.21	4 ± 0.19
Sugarcane bagasse	45 ± 0.52	26 ± 0.34	19 ± 0.13
Groundnut husk	36 ± 1.41	20 ± 0.88	25 ± 1.03

(Salihu *et al.*, 2015)

1.2.3 The Production of Furfural and Conversion Process

Furfural is an aldehyde as well as an organic solvent with the formula of $C_5H_4O_2$. It could be used to produce alkanes and furan through catalytic decarboxylation reactions of furfural (Chheda and Dumesic, 2007). Furfural (2-furaldehyde) is a heterocyclic aldehyde derived from acid hydrolysis and dehydration of pentoses (mainly xylose) sugars contained in lignocellulosic biomass fraction (Vazquez *et al.*, 2007). Furfural can be produced by one-step or two-steps conversion processes. In the one-step process, pentosans are hydrolyzed into xylose and then dehydrated into furfural simultaneously. However, in the two-step process, hydrolysis of pentosans occurs under mild conditions followed by the dehydration of xylose into furfural (Perego and Bianchi 2010; Serrano *et al.*, 2010).

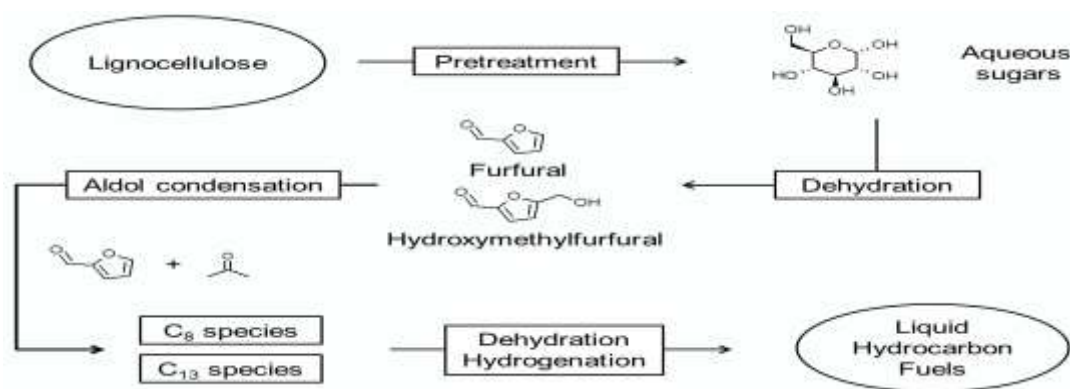


Figure 1.2: Chemical Transformation of Biomass to Liquid Hydrocarbon (Rong *et al.*, 2010).

Sokoto,*et al.*(2017) reported furfural production from millet husk via simultaneous hydrolysis and dehydration processes. Where the Furfural optimal yield of (71.55%) was achieved at 184⁰C,39 min, and 9% acid concentration. Jian *et al.* (2015) reported the optimal furfural of 78.5% from corncobs in a one-pot method catalyzed by ZSM-5 at 473 K, 30% ZSM-5, 15 mL of toluene, and 500mM of NaCl for 2 h. Also, Ong and Sashikala, (2007) obtained an optimal furfural yield of 75% from dry rice husk using 10% sulphuric acid for 7 h. The yield was obtained with heterogeneous catalysts in dimethyl sulfoxide (DMSO) and toluene/water solvents; however, the yield was significantly lower when water was used as a solvent. However, the furfural cannot be utilized as a motor fuel because of its tendency to polymerize (Diaz *et al.*, 2005). However, furfural can be hydrogenated to furfuryl alcohol, methyl furan, tetrahydrofurfural alcohol, and methyltetrahydrofuran (MTHF), which have octane number of 83, 74, 83, and 74, respectively (Huber *et al.*, 2005). Among the

hydrogenated forms of furfural, only MTHF is suitable as a motor fuel because it will not polymerize and has low volatility. Furfural can also be used to produce liquid alkanes ($n\text{-C}_7$ to C_{15}) using aqueous-phase hydrogenation and base-catalyzed aldol condensation step (Faba *et al.*, 2012).

1.2.4 Aldol Condensation

Aldol condensation is the reaction of carbonyl enolates with aldehyde and ketones to form β -hydroxy carbonyl when subsequently dehydrated form α - β unsaturated compounds. This reaction is one of the most powerful reactions that increase the C–C bonds.(Faba *et al.*, 2012). The extent of the addition reaction of two species containing carbonyl groups to form aldol adducts is controlled by equilibrium; however, dehydration is highly favorable and drives the reaction forward to form α , β -unsaturated compound. Aldol condensations are especially useful in biomass upgrading because the facile dehydration removes oxygen, increases the carbon to oxygen ratio, and assists in the conversion of biomass-derived oxygenate to liquid hydrocarbons (Gabriels *et al.*, 2015). Therefore, this coupling reaction is widely used to upgrade bio-derived carbonyl compounds to form larger products that can be converted into jet and diesel fuels or lubricants by subsequent hydrogenation (Anbarasan *et al.*, 2012).

Aldol condensations are generally carried out at mild reaction temperatures in the presence of a homogeneous or heterogeneous acid, base, or amphoteric catalyst such

as alkali metals, metal oxides, mixed metal oxides, hydroxyapatite, amines grafted onto supports, and metal-substituted zeolites (Kozlowski and Davis, 2013; Gabriels *et al.*, 2015). However, few studies have been reported for aldol-condensation using solid base catalysts in water, because the leaching of catalyst components into the water phase and poor hydrothermal stability pose significant challenges. Recent improvements in heterogeneous catalyst systems possessing acid-base bifunctionality showed greater reaction rates by stabilizing the transition states on the acid-base pair sites. Factors such as reaction temperature, reactant molar ratio, the structure of reactant molecules, and the nature of the catalyst determine the selectivity of the process toward heavier compounds (Climent *et al.*, 2002; Sankaranarayanapillai *et al.*, 2015). Faba *et al.* (2012) demonstrated the reaction network for aldol- condensation of furfural and acetone as shown in Figure 1.4.

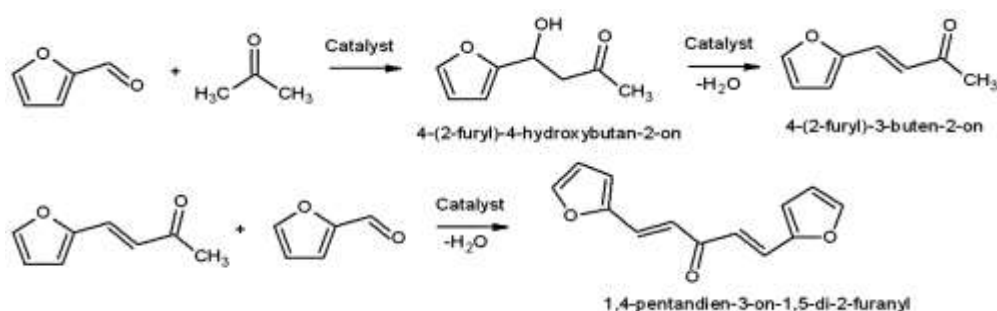


Figure 1.3: Step-wise reaction for aldol- condensation of furfural with acetone(Faba *et al.*, 2012)

1.2.5 Hydrotreating of Bio-Oil

Hydrodeoxygenation (HDO) of bio-oils involves treating bio-oils at moderate temperatures (200-400°C) with high-pressure H₂ in the presence of heterogeneous catalysts. However, the high H₂ consumption and capital costs and low product selectivity render this method uneconomical (Xiong *et al.*, 2011). Direct hydrogenation of bio-oil in batch reactors over Raney Ni (200°C, 40 bar H₂) yielded only 30% organic liquid indicating that the direct hydro-processing of bio-oils is difficult and produces a large yield of coke and tar, which lead to deactivation issues (Xiong *et al.*, 2011). One of the catalyst deactivation mechanisms that occur during the HDO of bio-oil is carbon deposition on the catalyst surface (Xiu and Shahbazi 2012). This deactivation represents a major limitation of this technology because the catalyst has to be frequently regenerated. One approach that has been reported is to try to develop HDO catalysts that have low acidity and hence a lower rate of coke formation (Huber *et al.*, 2006).

Elliott and co-workers have reported that two hydrogenation steps are typically required for HDO of pyrolysis oil: 1) a low-temperature step (100-140°C) and 2) a high-temperature step (200-300°C) with final products containing 40% of the starting carbon (Elliot and Hart, 2009). The purpose of the low-temperature step is to hydrogenate aldehydes and ketones and make the oil more stable. Low-temperature stabilization step does not completely deoxygenate the bio-oil. However, it does make the oil more stable and decreases the rate of coke formation in the high-temperature

HDO step. The improved stabilization of the resulting bio liquid by the low-temperature hydrogenation also allows the bio-oil to be easier to handle and store for further upgrading and applications in existing crude oil refinery settings (Huber *et al.*, 2006).

The current bio-oil hydro-deoxygenation state of the art indicates that there is a wide range of products formed and that the involved catalytic chemistry needs to be understood in more detail (Li *et al.*, 2011). Therefore, future work on hydrodeoxygenation could focus on developing non-sulfur-based catalysts for hydrodeoxygenation.

1.2.6 Statement of the Research Problem

Municipal solid waste (MSW), as it popularly called globally, comprised of all form organic wastes generated from agricultural activities, households, commercial activities among others. Most of these wastes end up in the landfill or in the environment creating serious havoc to the habitats as well as environmental degradation. With the rapid depletion of fossil fuels reserves with increasing demands and uncertainty in this supply, there is a need for sustainable means for abating these waste materials especially for the conversion of waste to wealth. Therefore, conversion of hemicellulose obtained from maize cobs into liquid fuels like gasoline and diesel is one of the forefront issues critically giving preference and it could be a profitable process to mitigate the menace of these organic wastes.

1.2.7 Justification of the Study

Production of liquid hydrocarbons from sorghum straw, rice husk, millet husk, corncobs and other lignocellulose biomass and the effect of reaction conditions have been reported by several kinds of literature (Vazquez *et.al.*, 2007; Ong and Sashikala, 2007; Li *et al.*, 2011; Jian *et al.*, 2015; Sokoto *et al.*, 2017). However, research on the production of liquid hydrocarbons has not been reported from maize cobs using NiO/Al₂O₃ as a catalyst.

Therefore, this work intends at providing another information on the production of liquid hydrocarbons from maize cobs and the potential of NiO/Al₂O₃ as hydrodeoxygenation catalyst

1.2.8 Aim and Objectives

The aim of this research is to produce liquid hydrocarbons from hemicellulose obtained from maize cobs *via* catalytic conversion.

The specific objectives of the research are to:

- i. Produce Furfural from maize cobs by acid hydrolysis and dehydration process
- ii. Determine the effect of reaction variables (temperature, time and acid concentration) on Furfural production using Taguchi Array Design.
- iii. Synthesize and characterize NiO/Al₂O₃ catalyst.

- iv. Convert the furfural into hydrocarbons by hydrodeoxygenation process
- v. Identify the chemical composition of the generated hydrocarbons using GC-MS

1.2.9 Scope and delimitation

The scope of this research is limited to the conversion of hemicellulose obtained from maize cobs to liquid alkanes (within gasoline and diesel range). However, the emphasis is to determine the effect of variables on Furfural production process and to study the nature of the liquid products. In addition, the research did not account for the optimization of other reaction stages and the gases that was produced during the process.

CHAPTER TWO

MATERIALS AND METHODS

2.1 Materials

Table 2.1: List of Chemicals Used in the Research

Chemicals	Chemical formula	Purity(%)	Grade	Manufacturer
Sulphuric acid	H ₂ SO ₄	98.0	A.R	British Drug House
Sodium chloride	NaCl	99.5	A.R	LOBA Chemie
Dichloromethane	CH ₂ Cl ₂	99.0	A.R	LOBA Chemie
Sodium sulphate	Na ₂ SO ₄	99.0	A.R	British Drug House
Sodium hydroxide	NaOH	97.0	A.R	Qaulikems
Furaldehyde	C ₄ H ₅ O ₂	98.0	A.R	British Drug House
Ethanol	C ₂ H ₅ OH	95.0	G.P.R	Kermel
Acetone	(CH ₃) ₂ CO	99.0	A.R	Beith Dekel
Ethyl acetate	CH ₃ COOC ₂ H ₅	99.5	A.R	JDL Industries
Hydratednickelnitrate	Ni(NO ₃) ₂ .6H ₂ O	99.9	A.R	Sigma-Aldrich
Alumina	Al ₂ O ₃	99.5	A.R	LOBA Chemie

Table 2.2: List of Instruments Used in the Research

Instruments	Model	Manufacturer
Analytical Balance	AW320	Shimadzu Japan
Magnetic Stirrer	ERC-1000H	Tokyo Rikakikai Co.Ltd, Japan
Reactor	SS316L	Fabricated in India
Rotary Evaporator	RE-200A	Xian Heb BioTec. CO. Ltd, China
Laboratory oven	SM9053	Surgifriend Med., England
FT-IR Spectroscopy	Carry630	Agilent Tech., USA
FT-IR Spectroscopy	MB3000	Agilent Tech., USA
GC-MS	1790B-5977A	Agilent Tech.

2.1.1 Sample Collection and Treatment

The sample (maize cobs) was obtained from Majema village opposite Nana Asama'u girl's hostel, Usmanu Danfodiyo University, Sokoto. The sample was sun dried at 39°C and stored at room temperature until required for the analysis.

2.2 Methods

2.2.1 Preparation of Reagents

a. Sulphuric Acid (H_2SO_4) Solution (10%)

The H_2SO_4 stock solution (10%) was prepared by dissolving 25. cm^3 of concentrated sulphuric acid in a beaker containing distilled water and the solution was transferred into 250 cm^3 volumetric flask and filled up the mark with distilled water. The solution was allowed to cool at room temperature.

b. Hydrated Nickel Nitrate ($\text{Ni}(\text{NO}_3)_2 \cdot 6\text{H}_2\text{O}$) Solution (0.6M)

Exactly 17.449g of nickel nitrate (II) was weighed and dissolved in 50 cm^3 of distilled water in a small beaker. The solution was transferred into 100 cm^3 volumetric flask and then brought to the mark with distilled water.

c. Sodium Hydroxide (NaOH) Solution (4M).

Exactly 16.000g was weighed and dissolved in 50 cm^3 of distilled water in a small beaker and the solution was transferred into 100 cm^3 volumetric flask and filled to the mark with distilled water

2.2.2 Catalyst Preparation

The catalyst was prepared by incipient wetness method of impregnation. 100 cm³ of 0.6M solution of Nickel (II) nitrate was added dropwise into the 200g of alumina powder (Al₂O₃) in the ratio of 1:2v/w with continuous mixing using magnetic stirrer for 10 min. The prepared slurry was placed in an oven to dry at 80°C for 8 h and then calcined in a furnace at 600°C for 4 h. The prepared catalyst (NiO/Al₂O₃) was stored at room temperature until required for the analysis (Francisco and Jesus, 2000).

Table 2.3: Furfural factors and their levels.

Factor	Levels
Temperature (°C)	140, 160, 180 and 200
Time (min)	20, 30, 40 and 50
Acid concentration (%)	4, 6, 8 and 10

2.2.3 Experimental Design

The experiments were designed using TAGUCHI design on MINITAB 17 Statistical Software. The effects of three factors i.e. temperature, time, and acid concentration at a different level were determined as indicated in Table 2.3 on yield.

2.2.4 Effects of variables:

Parameters considered for Furfural production include; temperature, time, and acid concentration as it was indicated in Table 2.3. The Taguchi array design was used in

this dissertation because it is the best method of experimental design having factors in four levels and above. The optimum parameters were determined for the highest yield of the furfural.

Table 2.4: Design of experiment (Taguchi Orthogonal Array Design)

Temperature(°C)	Time (min)	Acid conc.(%)
140	20	4
140	30	6
140	40	8
140	50	10
160	20	6
160	30	4
160	40	10
160	50	8
180	20	8
180	30	10
180	40	4
180	50	6
200	20	10
200	30	8
200	40	6
200	50	4

The optimum parameters which gave the highest yield of furfural were determined by using the equation below:

$$\% \text{Furfural Yield} = \frac{\text{Weight of Furfural formed (g)}}{\text{Dry weight of substrate utilized (g)}} \times 100$$

2.2.5 Production of Furfural

Plate 2.1 indicated a setup showing furfural production. Dried samples of 5.0 g and 5.0g of sodium chloride (NaCl) was mixed in a clean beaker. The mixture was placed into a 250cm³ borosilicate glass tube reactor and 50mL of 10% conc. sulphuric acid (H₂SO₄) was added. The reactor was placed upright inside the furnace and connected to water condenser. The distillation process was carried out according to the chosen variables of acid concentration, temperature and time respectively. The organic portion of the distillate was then extracted with dichloromethane using separating funnel and 0.2g of sodium sulphate was added to remove any trace water in the distillate. The solvent used was then removed using rotary evaporator at 40°C (Ong and Sashikala, 2007). Equation 2.1 was used to calculate the percentage yield of the furfural produced.



Plate 2.1 Setup Showing Furfural Production

2.2.6 Aldol Condensation

Setup showing aldol condensation of furfural with acetone was indicated on plate 2.2.

The reaction was performed in a flat bottom flask (250cm^3) reactor equipped with a magnetic stirrer. 10 cm^3 of the distillate (furfural) was mixed with 5 cm^3 of acetone in the ratio of 2:1 and then aqueous ethanol (50%) was added. The reactor was heated to 85°C , then 20 cm^3 of 4M NaOH was added into the mixture with vigorous stirring

(500 rpm/min) for 30 min (Fakhfakh *et al.*, 2008). After reaction time elapsed, the resultant mixture was filtered and washed three times with ethanol to remove the excess NaOH. The crystals obtained from the reaction was dissolved in ethyl.



Plate 2.2: Setup Showing Condensation of Furfural with Acetone

2.2.7 Hydrodeoxygenation

The hydrodeoxygenation (HDO) of the aldol product was carried out at 220°C in a stainless-steel tubular reactor. 30 cm³ of the aldol adduct and 1.8 g NiO/Al₂O₃ catalyst was heated in the reactor at 220°C for 1 hour under inert atmosphere and at 30 bars of Hydrogen. The liquid product obtained at the end of the reaction was then filtered and

analyzed using GC-MS (Faba *et al.*, 2015). Plate 2.3 below shows a setup of hydrodeoxygenation process.



Plate 2.3 Setup Showing Hydrodeoxygenation Process

a. FT-IR Spectroscopic and XRD Analysis

The Fourier transform infrared (FT-IR) spectroscopic analysis is used to quickly and definitely identify compounds such as compounded plastics, blends, etc. However, the FT-IR spectroscopy of standard furfural, catalyst prepared and produced furfural was carried out at Central Science Laboratory, Department of Pure and Applied Chemistry, Usmanu Danfodiyo University, Sokoto using Agilent Model and that of aldol adduct was carried out at Department of Chemistry, Yobe State University,

Damaturu using Agilent Technology model. The transmission rate was set at the range of 4000-650 cm^{-1} at 4 resolution value. The sample was mixed with alkali halide potassium bromide (KBr) and compressed into a thin transparent pellet using hydraulic press and placed in a standard sample compartment of the spectrometer and spectral data was obtained. The X-ray diffraction of prepared catalyst was carried out by Empyrean intelligent diffractometer model, Malvern Panalytical, Netherland at National Geosciences Research Laboratory, Nigerian Geological Survey Agency, Kaduna,

d. GC-MS Method of Analysis

GC-MS is extensively used for the analysis of these compounds which includes esters, fatty acids, alcohols, aldehydes, terpenes etc. The analysis of the hydrodeoxygenation product was carried out using GC/MS machine at chemistry central laboratory, Yobe State University, Damaturu. The GC 7890B, MSD 5977A, Agilent technology was equipped with a capillary column (30.0 m in length \times 250 μm in diameter \times 0.25 μm in film thickness). The injection volume was 1 μl and the inlet temperature was maintained at 250 $^{\circ}\text{C}$. The GC oven temperature was programmed initially at 70 $^{\circ}\text{C}$ for 1 min and then programmed to 260 $^{\circ}\text{C}$ at the rate of 10 $^{\circ}\text{C}$ per minute and held at 260 $^{\circ}\text{C}$ for 5 minutes. The front inlet temperature of the oven was 250 $^{\circ}\text{C}$ (pulsed split less-mode). The carrier gas was helium with a flow rate of 18 cm^3/min , pressure 4.9693 psi and septum purge flow 3 mL/min . The ionization mode was set at 70eV. Total Ion Count (TIC) was used to evaluate for compound identification and quantitation. The spectrum of the separated compound was compared with the database of the spectrum of known compound saved in the NIST02 Reference Spectral Library.

CHAPTER THREE

RESULTS AND DISCUSSIONS

3.1 Results

The results obtained from Furfural produced was presented in Table 3.1. An appreciable yield of furfural was achieved at the optimum condition of temperature, time and acid concentration. Taguchi array design was used to develop a correlation between condition variables of Furfural yields. The yield of furfural from hydrolysis and dehydration process of hemicellulose obtained from maize cobs was designed using TAGUCHI design on MINITAB 17 Statistical Software. The effects of three factors i.e. temperature, time, and acid concentration at a different level were determined and the effect of variables revealed furfural yield within the range of 15.0–72.00%. Contour plots were used to analyze the interactions between the corresponding variables on the furfural yield.

Table 3.1: Effects of Variables on the Furfural Production and the Yield Obtained

Temperature (°C)	Time (min)	Acid concentration (%)	Yield (%)
140	20	4	15
140	30	6	21
140	40	8	34
140	50	10	51
160	20	6	31
160	30	4	22
160	40	10	59
160	50	8	50
180	20	8	33
180	30	10	72
180	40	4	37
180	50	6	56
200	20	10	54
200	30	8	52
200	40	6	49
200	50	4	44

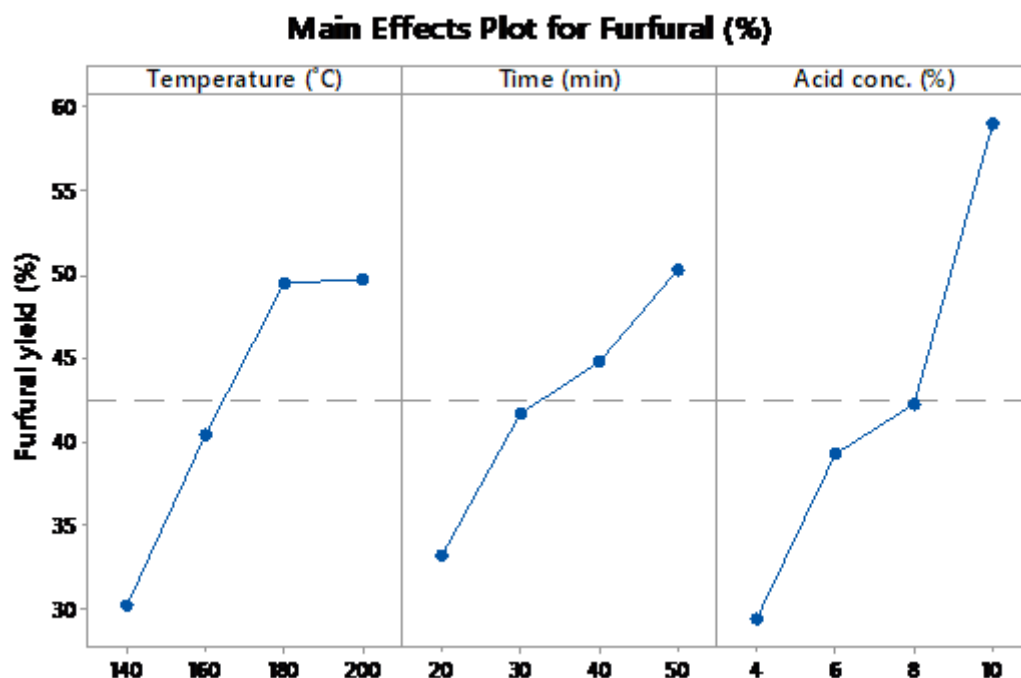


Fig. 3.1: Effects of Variables on the Furfural Yield

I. Effect of Temperature on the furfural yield

The experimental results illustrated in Figure 3.1 showed the Effect of Temperature on the furfural produced. It can be observed that the average Furfural yield significantly increases with increase in temperature from 140 to 200°C with yields of 30.5 to 49.75 this is due to the fact that the response surface of Furfural yield increases rapidly with an increase in reaction temperature within the range of 140-180°C. The yield of Furfural was noticed significantly increased between 140 to 180°C but the increase was slightly between 180 to 200°C which is in line with findings by Sokoto *et al.* (2017) where the temperature reached saturation point with the reaction time which virtually makes reaction difficult to proceed, thereby decreasing in the Furfural yield.

II. Effect of the time on furfural yield

The experimental results illustrated in Figure 3.1 shows that the time has also effect on the furfural produced. It can be observed that as the time increases from 20 minutes to 30 minutes the mean of the Furfural yield rapidly increases to about 41.75%. As the time continues to increase subsequently by 10 minutes the mean of the Furfural significantly increased to about 50.25%, simultaneously, which is in line with the findings of Amir *et al.*(2015).

III. Effect of acid concentration on furfural yield

In the study results presented in Figure 3.1, as the acid concentration increases from 4 to 6% the average mean of the Furfural yield significantly increases to 39.25% and subsequently increases to 59% with an increase in acid concentration from 6-10%. However, the percentage yield of furfural could be increased by increasing the concentration of sulphuric acid (Amir *et al.*, 2015).

Table 3.2: Analysis of Variance (ANOVA) for Furfural Production

Sources	DF	Adj ss	Adj ms	F- Value	P- Value
Temp. (°C)	3	1022.5	340.83	8.21	0.015
Time(min)	3	605.0	201.67	4.86	0.048
Acid Conc. (%)	3	1807.5	602.50	14.52	0.004
Error	6	249.0	41.50		
Total	15	3684.0			

Table 3.3: Model Summary

S	R-sq	R-sq (adj)	R-sq (pred)
0.644205	0.9334%	0.8310%	0.5194%

The Taguchi array design in Minitab Statistical tool was able to function as an optimal design for the desired response based on the model obtained and input criteria. The effect of variables of furfural yield was carried out based on the three variables i.e temperature, time and acid concentration which are in four different levels of 16 experimental runs. The general linear model was carried out to fit the response variable and investigate the variable that is significant and insignificant.

The “P” value less than 0.05 indicated that the particular term was statistically significant and “P” value greater than 0.05 indicated that the particular term was statistically insignificant. The “R²” (correlation coefficient) is the variability of the factors around the mean which explain how close the data are to the fitted regression line. That 0% means the model explains none of the variability and 100% indicates that the model explains all the of the variability of the response data around the mean. The “R²” (correlation coefficient) of the analysis was found to be 93.24% which showed that the variable fit the model. The analysis shows the temperature (0.015), time (0.048) and acid concentration (0.004) are less than 0.05 and therefore found to be statistically significant (Table 3.2)

3.2 Effect of Process Variables

Interaction plot of the variables at each level of another factor was plotted to examine whether the factors interact and to predict the optimum levels of each variable for maximum yield. The optimum conditions for maximizing Furfural yield were reaction temperature of 180°C for 30min reaction time and 10% acid concentration. The maximum response value of Furfural yield was obtained at 72.0% and the plot of

Furfural indicated that Furfural yields increased with an increase in reaction temperature in the range of 140-200°C. However, reaction temperature, reaction time and acid concentration had a linear individual significant influence on the Furfural yield.

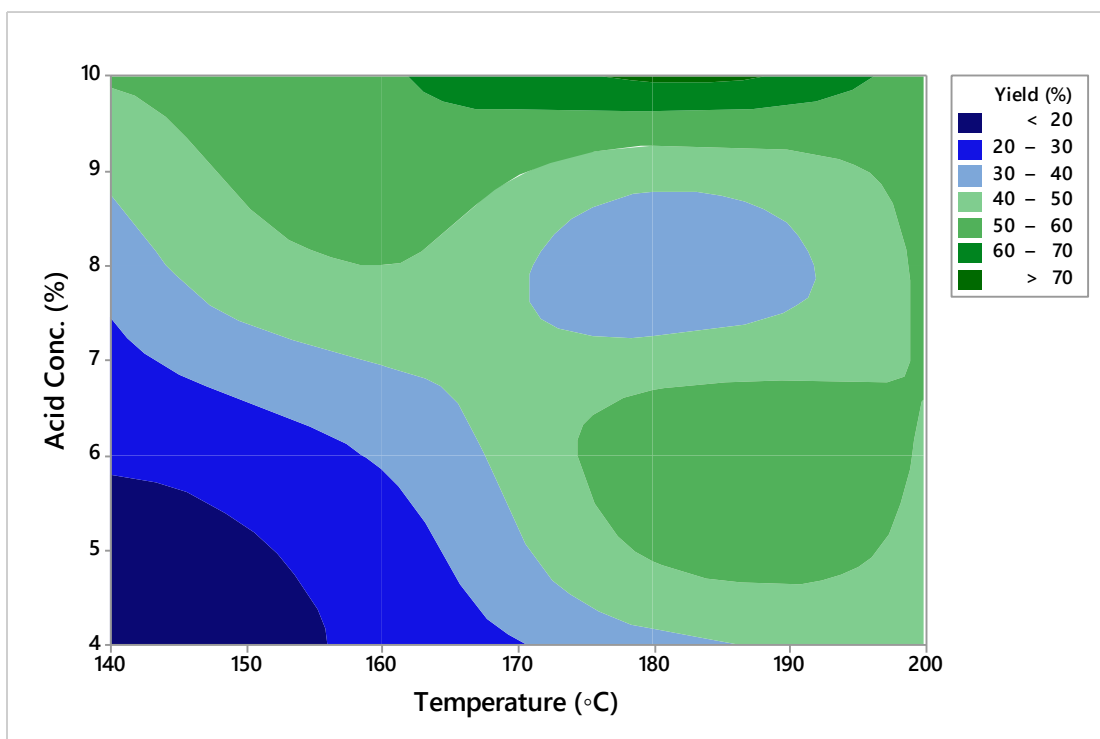


Fig 3.2: Effect of Temperature Against Acid Concentration on Furfural Yield

Figure 3.2 The experimental results illustrated in Figure 3.2 shows that the effect of Temperature against the acid concentration on the Furfural produced. It can be observed that there is an interaction between reaction temperature at different levels of acid concentrations. The average Furfural yield of less than 20, 20-30, 30-40 and 40-50% was obtained at 150°C, 160°C, 170°C and 180°C reaction temperature respectively, at 4-10% acid concentration. However, the maximum Furfural yield of 72% was noticed at 180°C and 10% acid concentration which is in line with the findings of Sokoto *et al.*, (2017).

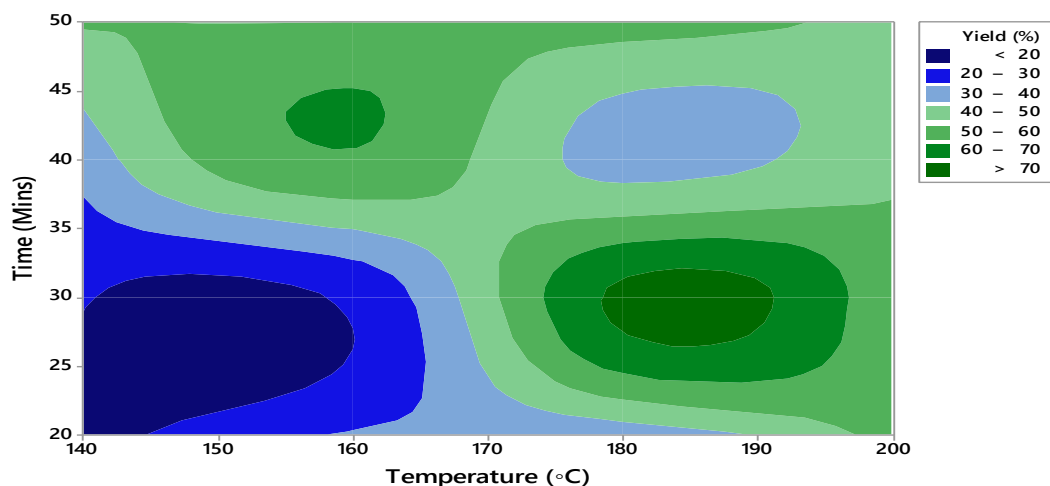


Figure 3.3: Effect of Temperature Against Time on Furfural Yield

From Figure 3.3, it is observed that when the reaction was performed at a reaction temperature of 160°C the Furfural yield slowly increases to 60-70% with an increase in reaction time of 45 minutes. Beyond this reaction time with an increase in reaction temperature, there is a slight decrease in furfural yield to about 50-60 % and that the optimum Furfural yield of greater than 72% was achieved at 30 minutes reaction time and 180°C reaction temperature. It is observed that the highest Furfural yield of 72% was achieved at reaction temperature at high of 180°C and at an average reaction time of 30 minute which is in line with the findings of Sokoto *et al.* (2017).

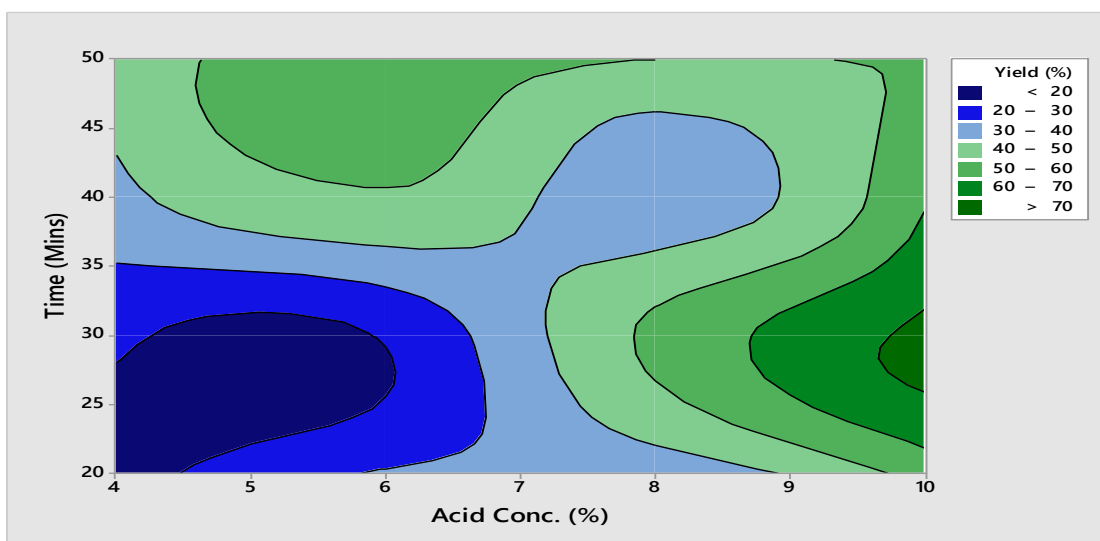


Fig 3.4: Effect of Time Against Acid Concentration on Furfural Yield

The experimental results illustrated in Figure 3.4 shows that time and acid concentration have an effect on the Furfural produced. It can be observed that from 4-9 % acid concentration the Furfural yield increases significantly with an increase in reaction time until the reaction reached equilibrium. Beyond the optimum reaction time with acid concentration, the reaction starts to progress in a backward direction towards reactants which is in line with the findings of (Samart *et al.*, 2009). The optimum yield of 72% was obtained at 30 minutes reaction time and 10% of acid concentration. The high percentage of acid concentration rapidly promote the production of Furfural yield. A similar result at optimum reaction time and acid concentration were obtained by Sokoto *et al.* (2017).

3.3 Identification of Furfural

The FT-IR assignment of functional groups to the produced furfural was shown in Table 3.4

Table 3.4: FT-IR Spectral Analysis of the Produced and Prepared Furfural

Group	Functional	Observed Frequencies cm^{-1}		Assignment
Frequencies cm^{-1}	Group	Standard Furfural	Observed Furfural	
1780-1670	C=O	1988	1690	Aldehyde
2900-2700	C-H	2848-2814	2848-282	
3100-3000	C-H	-	-	Aromatic
1600-1450	C=C	1570-1460	1570-1460	
1300-1000	C-O	1200-1000	1200-1000	Ether

The (Appendix II), shows the infrared spectrum of Furfural produced. The IR spectrum(Appendix II) shows a strong/sharp absorption 1690 cm^{-1} which corresponds to the absorption of conjugated carbonyl (C=O). The C=O absorption is lower than the usual absorption of aldehyde due to internal hydrogen bonding which occurs in conjugated unsaturated aldehyde and conjugation lower the vibrational frequency of carbonyl compounds. Similarly, C=O absorption was also observed in the standard furfural spectrum (Appendix III). The presence of the aldehyde group was proven with the existence of two weak absorption gained at 2848 cm^{-1} and 2812 cm^{-1} as observed in the standard furfural that indicated moderate intense stretching of aldehydic C-H which is attributable to Fermi resonance between the fundamental aldehydic C-H stretching and the first overtone of the aldehydic C-H bending vibration. In addition, no peaks were observed at $2100\text{--}2260\text{ cm}^{-1}$ as observed in the standard furfural spectrum that could be due to the presence of other compounds in the furfural standard. Strong peaks indicated from 1570 cm^{-1} to 1466 cm^{-1} are inactive of stretching of C=C from the aromatic ring and strong peaks at 1020 cm^{-1} indicated the C-O stretching vibration in both the standard and the produced furfural. Also, there is lower broad absorption at 3462 and 3540 cm^{-1} could be due to the presence of O-H vibration which could be attributed to the absorption of the solvent that remains in the product. This IR spectrum was also compared with that of the standard furfural spectrum (Appendix II) and the one published by Ong and Sashikala (2007).

3.4 Analysis of the Aldol Adducts

The result for the characterization of aldol adduct using FT-IR was shown in Table 3.5 and the peak for each absorption was assigned.

Table 3.5: FT-IR Spectral Analysis of the Aldol Adducts

Group	Functional	Observed Frequencies	Assignment
Frequencies cm ¹	Group	cm ⁻¹	
1700-1725	C=O	1584	Ketones
3080-3140	C-H	3055-3141	Alkenes
1630-1670	C=C	- -	
3000-3100	C-H	- -	Aromatic
1450-1600	C=C	- -	
1000-1300	C-O	1199-1240	Ether

The IR spectrum (Appendix VIII) of Furfural-Acetone dimer obtained was recorded (Table 3.5). The frequency of the main absorption bands illustrated that the (C–H) vibrational frequency appears at 3055 and 3141 cm⁻¹ correspond to the sp² vibration in the furan ring. The stretching absorbance(C=O) was observed at 1584 cm⁻¹ infers the carbonyl group and a sharp stretching absorbance band at 1199 cm⁻¹ and 1240 cm⁻¹ probably indicates C-O stretching for cyclic C-O-C linkage of furfural. Also, there is lower broad absorption at 3462 and 3540 cm⁻¹ could be due to the presence of O-H vibration which could be attributed to the absorption of the solvent that remains in the product. The spectrum observed was in line with the findings by Gandini, (2010).

3.5 Catalyst Characterization

i. *Fourier-transform infrared spectroscopy (FTIR)*

NiO/Al₂O₃ has been successfully synthesized. Infrared spectroscopy was used for the characterization of inorganic compound (Francisco and Jesus, 2000). The (Appendix

VII) shows the infrared spectrum of NiO/Al₂O₃ from hydrated nickel and alumina. Which shows a vibrational peak in the range of 400-650 cm⁻¹ representing the characteristic metal-oxygen stretching frequencies associated with the vibrations of Ni-O-Al-O and Ni-O-Al bonds. A sharp peak can be seen around 469 cm⁻¹ the infrared spectrum corresponds to functional group Ni-O stretching frequency synthesized from nickel nitrate which corresponds with the findings of Sokoto *et al.* (2017). The Ni-O peak intensity reduced as nickel nitrate was decomposed to nickel oxide (Galván- Ruiz *et al.*, 2009). Upon calcination, the nickel nitrate was thermally decomposed into oxide and losses nitrate. Thus, this leads to the loss of characteristics of peaks of nitrates on the Infra-red spectrum on the synthesized nickel oxide over alumina. The reduced intensity of absorption band which corresponds to nitrates can be seen at, 520 cm⁻¹, 500cm⁻¹ and 450 cm⁻¹ on the IR spectrum of nitrate oxide from NiO/Al₂O₃.

The absorption peaks at 610 cm⁻¹ of the infra-red spectrum were due to the Al-O stretching frequencies. The characteristic absorption of NiO/Al₂O₃ observed corresponds to the absorption of NiO/Al₂O₃ reported by Ryzkowski *et al.* 2006)

ii. X-ray diffraction (XRD)

The X-ray diffraction pattern of as-synthesized catalyst and calcined powder of NiO and alpha Al₂O₃ nanoparticles are shown in the appendix (V) and appendix (VI) respectively. The diffraction peaks are sharp and broad due to the medium size effect and reflection peaks from the combustion (Sarika *et al.*, 2016). The XRD pattern as obtained NiO, which shows peaks arising from NiO indicating that combustion is incomplete. The combustion of this residual occurs during subsequent calcination at 600°C for 4 hours and phase pure cubic NiO was obtained. The calcined powder has

crystallographic parameters of Fm-3m space group, 225 space group number and lattice parameter of 4.178Å. On the other hand, the as-obtained Al₂O₃ is amorphous. It needs high calcination temperature to obtain crystalline alpha Al₂O₃ particles (Sarika *et al.*, 2016). Therefore as-obtained powder was calcined at 600°C for 4 h. Its XRD pattern shows sharp peaks indicating the presence of small size particles. The crystallographic parameters indicated the crystal system of the rhombohedral, space group of R-3c, space group number of 167 and lattice parameter of a=b=4.7590 and c=12.9965Å. The elemental analysis of the calcined powders also showed no impurities were detected due to neither Ni and oxygen or Al and oxygen. This is in line with the findings of (Sarika *et al.*, 2016).

Table 3.6: The Crystallographic Parameters of NiO and Al₂O₃ Phases

Parameters	Calculated density (g/cm ³)	Measured density (g/cm ³)	Volume of the cell (10 ⁶ pm ³)
NiO	6.80	-	72.93
Al ₂ O ₃	3.98	3.99	254.91

3.6 Analysis of the Hydrodeoxygenated Products

The chemical compositions of hydrodeoxygenation products over NiO/Al₂O₃ catalyst analyzed using GC-MS are presented in Table 3.7

Table 3.7: Compositions of Hydrodeoxygenated Products

Peak	Name of compounds	RT (min)	Formula	% Relative peak
1	Heptane	9.708	C ₇ H ₁₆	28.06
2	Nonane	10.034	C ₉ H ₂₀	7.83
3	Decane	10.154	C ₁₀ H ₂₂	17.65

Result in Table 3.7 shows the distribution of alkanes obtained from hydrodeoxygenation of aldol adducts. The products were mainly liquid hydrocarbons within the carbon range of (C₇ – C₁₅). The presence of pentadecene indicated partially hydrogenation which might require further hydrogenation. The total relative peak area of the products was 61.08% with heptane and decane being the major products, each of which accounted for 28.06% and 17.65% respectively. Based on GC–MS data, the liquid phase also contains significant amounts of other alkanes which could be formed due to decomposition and polymerization reaction. In the liquid phase, other than alkanes, there were some other organic oxygenates identified by GC–MS, including methanol and acetic acid which are most likely byproducts.

CHAPTER FOUR

CONCLUSION AND RECOMMENDATIONS

4.1 Conclusion

The conversion of maize cobs to liquid hydrocarbons *via* aqueous phase process using NiO/Al₂O₃ as catalyst revealed that:

- i. Furfural was successfully produced *via* aqueous phase hydrolysis and dehydration processes
- ii. Optimization of furfural production was successfully achieved at 180°C reaction temperature 30 min reaction time and 10% acid concentration revealing the highest yield of 72.0% obtained
- iii. The prepared catalyst (NiO/Al₂O₃) showed significant improvement in its catalytic activity by lowering reaction time and producing a significant amount of bio-oil.
- iv. Appreciable quantity of hydrocarbons was generated by aqueous-phase processing of maize cobs
- v. A result from GC-MS analysis confirmed the presence of alkanes (within the range of C₇ -C₁₅)

4.2 RECOMMENDATIONS

From the highlight of this study, the following recommendation were made:

- i. The optimization of aldolic condensation of furfural on acetone should be studied by maximizing the chemical yield of Furfural with Acetone.

- ii. Different metallic catalyst should be tested in the hydrodeoxygenation process to ascertain the activity of the different catalyst and to identify which catalyst gives the best result
- iii. Solid acid catalyst should be used in the production of furfural to improve the yield and avoid the problems associated with a homogeneous acid catalyst.
- iv. The use of a single reactor and catalyst should be adopted in the condensation and hydrodeoxygenation process to reduce the cost of the process and reaction steps involved.

REFERENCES

- Amir, S., Ayyaz, M., Shahid, S., Ziad, A., Saeed, H.M.U. and Umar, F. (2015). Effect of acid concentration on the extraction of furfural from corn cobs, *International Journal of Chemical Engineering and Applications*, **6**(5), 281-283.
- Anbarasan, P., Baer, Z. C., Sreekumar, S., Gross, E., Binder, J. B., Blanch, H. W., Clark, D. S., and Toste, F. D. (2012). Integration of Chemical Catalysis with Extractive Fermentation to Produce Fuels. *Nature*, **491**, 235–239.
- Barrett, C. J., Chheda, J. N., Huber, G. W. and Dumesic, J. A. (2006). Single-Reactor Process for Sequential Aldol-Condensation and Hydrogenation of Biomass-Derived Compounds in Water, *Applied Catalysis*, **66**(1-2), 111-118.
- Bobleter, O. (1994). Hydrothermal degradation of polymers derived from plants. *Prog. Polym. Sci.* **19**, 797–841.
- Bond, J. Q., Alonso, D. M., Wang, D., West R. M and Dumesic, J. A. (2010). Integrated Catalytic Conversion of γ -Valerolactone to Liquid Alkanes for Transportation Fuels. *Science*, **327**, 1110–1114.
- Brunner, G. (2009). Near critical and supercritical water. Part I. Hydrolytic and hydrothermal processes. *J. of Supercrit Fluids*, **47**, 373-381.
- Chheda, J. N. and Dumesic, J. A. (2007). An Overview of Dehydration, Aldol-Condensation and Hydrogenation Processes for Production of Liquid Alkanes from Biomass-Derived Carbohydrates. *Catalysis Today*, **123**, 59–70.
- Choudhary, V., Sandler, S. I., and Vlachos, D. G. (2012). Conversion of Xylose to Furfural Using Lewis and Bronsted Acid Catalyst in Aqueous Media, *Advanced Synthesis Catalysis*, **2**(9), 2022-2028.
- Climent, M. J., Corma, A., Iborra, S., and Velty, A. (2002). Synthesis of Methylpseudoionones by Activated Hydrotalcites as Solid Base Catalysts, *Green Chemistry*, **4**, 474–480.
- Demirbas, M. (2006). Current Technologies for Biomass Conversion into Chemicals and Fuels. *Energy Sources Part a – Recovery Utilization and Environmental Effects*, **28**, 1181–1188.
- Diaz, A. S., Pillinger, M. and Valente, A. A., (2005). Dehydration of Xylose into Furfural over Micro-mesoporous Sulfonic Acid Catalysts. *Journal of Catalysis*, **229**, 414-423.
- Elliott, D. C. and Hart, T. R. (2009). Catalytic hydroprocessing of Chemical Models for Bio-Oil Catalytic, *Energy Fuel*, **23**, 631-637.
- Faba, L., Diaz, E. and Ordonez, S. (2012). Aqueous-Phase Furfural-Acetone Aldol Condensation over Basic Oxides. *Applied Catalysis B*, **113**, 201.

- Faba, L., Diaz, E., Vega, A. and Ordonez, S. (2015).Hydrodeoxygenation of Furfural-Acetone Condensation Adducts to Tridecane over Platinum Catalysts, *Catalysis Today*,**269**, 132-139.
- Fakhfakh, N., Cognet, P., Cabassud, M. Y.and Rioios, M. D. (2008). Stoichio-Kinetic Modeling and Optimization of Chemical Synthesis: Application to the Aldolic Condensation of Furfural on Acetone. *Chemical Engineering Process*,**47**(3), 349–362.
- Falkehag, S. I. (1975). Synthesis of a phenolic polymer. *Applied Polymer*,**28**, 247-257.
- Francisco M. and Jesus E.S. (2000). Simple Synthesis and Characterization of Several Nickel Catalytic Precursors,*Journal of Chemical Education*, **79**(4), 489.
- Gabriels, D., Hernandez, W. Y., Sels, B., Voort, P. V. and Verberckmoes, A. (2015) Review of Catalytic Systems and Thermodynamics for the Guerbet Condensation Reaction and Challenges for Biomass Valorization,*Catalysis Science and Technology*, **5**, 3876–3902.
- Galván-Ruiz, M., Hernández, J., Baños, L., Noriega-Montes, J., Mario, E. and Rodríguez, G. (2009). Characterization of Calcium Carbonate, Calcium Oxide, and Calcium Hydroxide as Starting Point to the Improvement of Lime for their Use in Construction,*Journal of Materials in Civil Engineering*, **21**(11), 694–698,
- Gandini, A. (2010). Furans as Offspring of Sugars and Polysaccharides and Progenitors of a Family of Remarkable Polymers: A Review of Recent Progress. *Polymer Chemistry*,**1**, 245
- Gurbuz E. I., Alonso, D. M., Bond, J. Q. and Dumesic J. A. (2011). Reactive Extraction of Levulinate Esters and Conversion to γ -Valerolactone for Production of Liquid Fuels,*Chemical and Sustainability*, **4**(3), 357-361.
- Hideshi H. (2004). Solid base catalyst: generation, characterization and catalytic behavior of basic sites, *Journal of the Japan Petroleum Institute*,**47**(2), 67-81.
- Hongjun, D., Wenwen, T., Zongjie, D., Liejian, Y., Fuyu, G., Yangping, Z. and Yin, L. (2011). Biobutanol, *Advance Biochem Enginering/Biotechnol*,**1**(16). 23-25
- Huber, G. W., Chheda, J. N., Barrett, C. J. and Dumesic, J. A. (2005). Production of Liquid Alkanes by Aqueous-Phase Processing of Biomass-Derived Carbohydrates, *Science*,**308**(57), 1446-1450.
- Huber, G.W., Iborra, S. and Corma, A. (2006). Synthesis of Transportation fuels from biomass: Chemistry, catalysts, and engineering. *Chemical Review*,**106**, 4044-4098.
- Iken, J.E. and Amusa, N.A. (2004). Maize research and production in Nigeria, *African Journal of Biotechnology*, **3**(5), 302-307.

- Jian, D., Hongling, G., Jing, G., Guang, Y., Yuedong, Z., Haisong, W. and Xindong, M. (2015). Furfural formation from Corn Cobs in a one-pot method catalyzed by ZSM-5, *International Conference on Advances in Energy and Environmental Science*, 808-812.
- Kaygusuz, K., Coskun, A. A. and Toklu, E. (2015). Energy from biomass-based waste for sustainable energy development, *Journal of Engineering Research and Applied Science*, **4**(2), 307-316
- Kozlowski, J.T. and Davis, R. J. (2013). Heterogeneous Catalysts for the Guerbet Coupling of Alcohols. *Advanced Synthesis and Catalysis*, **3**, 1588–1600.
- Kumar, S., (2010). Hydrothermal Treatment for Biofuels: Lignocellulosic Biomass to Bioethanol, Biocrude, and Biochar (Thesis), Auburn University, Auburn, Alabama, p. 239
- Li, N., Tompsett, G. A., Zhang, T., Shi, J. Wyman, C. E. and Huber, G. W. (2011). Green gasoline from aqueous phase hydrodeoxygenation of aqueous sugar solutions prepared by hydrolysis of maple wood, *Green Chemistry*, **13**, 91-101.
- Liu, H. H, Liu, X. H, Wang, Y. Q. and Lu, G. Z. (2008). An optimum condition study on condensation of furfural and acetone by homogeneous catalysis of ammonia. *Industrial Catalysis*, **16**(2), 32–36.
- Linda Campbell Franklin (2013). Corn in Andrew F. Smith (ed). The oxford encyclopedia of food and drink in America. 2nd ed. Oxford: Oxford University Press, 551- 558.
- Massimo, B., Claudio, F., Mariangela, S., Carlo, F., and Amedeo, R. (2016). The use of cobs, a by-product of maize grain, for energy production in anaerobic digestion, *Italian Journal of Agronomy*, **11**(754).
- Mehdi, H., Fabos, V., Tuba, R., Bodor, A. and Mika, L. T. (2008). Integration of homogeneous and heterogeneous catalytic processes for a multi-step conversion of biomass: from sucrose to levulinic acid, γ -Valerolactone, 1,4-Pentanediol, 2-methyl-tetrahydrofuran, and alkanes, *Green Chemistry*, **10**, 238
- Merlo, A. B., Vetere, V., Ruggera, J. F and Casella, M. L. (2009). Bimetallic PtSn catalyst for the selective hydrogenation of furfural to furfuryl alcohol in liquid-phase. *Catalysis Communication*, **19**, 1665-1669.
- Oladejo, J. A. and Adetunji, M. O. (2012). Economic analysis of maize (zea mays L.) production in Oyo state Nigeria, *Agricultural Science Research Journal*, **2**(2), 77-83.
- Olsson, L., Jorgensen, H., Krogh, K. B. R., and Roca, C. (2005). Bioethanol production from lignocellulosic material in Polysaccharides: Structural diversity and functional versatility, 2nd edition, Dumitriu, Marcel Dekker, 957-993.

- Ong, H.K. and Sashikala, M. (2007). Identification of furfural synthesized from pentosan in rice husk, *Journal of Tropical Agriculture and Food. Science*, **35**(2), 305–312.
- Pastircakova, K. (2004). Determination of trace metal concentrations in ashes from various biomass materials. *Energy Edu. Sci. Technol*, **13**, 97-104.
- Pavia, D. L., Lampman, G. M. and Kriz, G. S (2001) Introduction to Spectroscopy, Third Edition. Published by Thomson Learning Inc. ISBN: 0-03-031961-7
- Perego, C. and Bianchi, D. (2010). Biomass upgrading through acid-base catalysis. *Chemical Engineering Journal*, **161**, 314-322.
- Roman, L. Y. and Dumesic J. A. (2009). Solvent effects on fructose dehydration to 5-hydroxymethylfurfural in biphasic systems saturated with inorganic salts *Topics in Catalysis*, **52**, 297-303.
- Rong, X., Ayyagari, V. Subrahmanyam, H. O., Wei, Q., Peter, V. W., Hemant, P. and Huber, G. W. (2010). Production of Jet and Diesel Fuel Range Alkanes from Waste Hemicellulose-Derived Aqueous Solutions, *Journal of the royal society of chemist*, **140**, 77-84.
- Ryczkowski, J., Pasieczna, S., Stolecki, K. and Borowiecki T., (2006). FT-IR/PAS characteristic of the Ni-NiO/Al₂O₃ catalyst, *Journal de Physique IV France*, **137**, 325-329.
- Salihu, A., Abbas, O., Sallau, A. B. and Alam, M. Z. (2015). Agricultural residues for cellulolytic enzyme production by *Aspergillus niger*, Effect of Pretreatment, *Biotechnology*, **5**(6), 1101-1106.
- Samart, C., Sreetongkittikul, P. and Sookman, C. (2009). Heterogeneous catalysis of transesterification of soybean oil using KI/mesoporous silica, *Fuel Processing Technology*, **90**(7-8), 922–925.
- Sankaranarayanapillai, S., Sreekumar, S., Gomes, J., Grippo, A., Arab, G. E., Head-Gordon, M., Toste, F. D., and Bell, A. T. (2015). Catalytic upgrading of biomass-derived methyl ketones to liquid transportation fuel by an organocatalytic approach. *Angewandte Chemie International Edition in English*, **54**, 4673–4677.
- Santos, F., Colodette, J. and Queiroz, J.H. (2013). Bioenergia e biorrefinaria cana-de-açúcar e espécies florestais, **99**, 234-254.
- Sarika, P.P., Jadhav, L.D., Dubal, D.P. and Puri, V.R. (2016). Characterization of NiO-Al₂O₃ composite and its conductivity in biogas for oxide fuel cell, *Material Science Poland*, **34**(2), 266-274.

- Serrano, L., Eguees, I., Alriols, M. G., Llano-Ponte, R., and Labidi, J. (2010). Miscanthus Sinensis fractionation by different reagents, *Chemical engineering journal*, **156**, 49-55.
- Shaw, R. H. 1988. Climate requirement. In: Sprague G.F., Dudley J.W eds. Corn and Corn 638 Improvement, 3rd ed Madison, WI:ASA 609.
- Sokoto, A. M., Ibrahim, S. M., Dangoggo, S. M., Anka N. U. and Hassan, L.G. (2017). Optimization of furfural production from millet husk using response surface methodology, *Utilization, Environmental Effects*, **40**(1), 120-124.
- Soni, S.W., Armansyah, H. T., Martin, D., Hiroshi N. (2008). The effect of palm biodiesel fuel on the performance and emission of the automatic diesel engine, *agricultural engineering international, CIGR Ejournal*, **(7)**5.
- Tusher, M. S. (2010). Pyrolysis of flax straw: Characterization of char, liquid and gas. (Thesis). Retrieved from ProQuest Dissertations and Theses, University of Regina. University of Regina, Saskatchewan, Canada. p. 111
- Vazquez, M., Oliva, M., Téllez-Luis, S. J. and Ramírez, J. A. (2007). Hydrolysis of Sorghum Straw using Phosphoric Acid: Evaluation of Furfural Production. *Bioresource Technology*, **98**, 3053–3060.
- West, R. M., Liu, Z. L., Peter, M. and Dumesic, J. A., (2008). Liquid alkanes with targeted molecular weights from biomass-derived carbohydrates, *Chemistry and Sustainability*, **1**, 417-424.
- Wyman, C. E., Decker, S. R., Himmel, M. E., Brady, J. W., Skopec, C. E. and Viikari, L., (2005). In *Polysaccharides*, 2nd ed.; Dumitriu, S., Ed.; Marcel Dekker: New York. Available online at <http://www.sciencedirect.com/science/article>.
- Xiong, W. M., Fu, Y., Zeng, F. X. and Guo, Q. X. (2011). An in-situ reduction approach for bio-oil hydroprocessing fuel process, *Technology*, **92**, 1599-1605.
- Xiu, S. and Shahbazi, A. (2012). Bio-oil production and upgrading research, *Renewable and Sustainable Energy Reviews*, **16**, 4406-4414.
- Zahra Khodarahmpour (2012). Morphological classification of maize (zea mays L.) genotype in heat stress condition, *Journal of Agricultural Science*, **4**(5).

APPENDICES

APPENDIX I:

General Linear Model: Furfural yield (versus Temperature (°C), Time (min), Acid concentrati

Method

Factor coding (-1, 0, +1)

Factor Information

Factor	Type	Levels	Values
Temperature (°C)	Fixed	4	140, 160, 180, 200
Time (min)	Fixed	4	20, 30, 40, 50
Acid concentration(%)	Fixed	4	4, 6, 8, 10

Analysis of Variance

Source	DF	Adj SS	Adj MS	F-Value	P-Value
Temperature (°C)	3	1022.5	340.83	8.21	0.015
Time (min)	3	605.0	201.67	4.86	0.048
Acid concentration(%)	3	1807.5	602.50	14.52	0.004
Error	6	249.0	41.50		
Total	15	3684.0			

Model Summary

S	R-sq	R-sq(adj)	R-sq(pred)
6.44205	93.24%	83.10%	51.94%

Coefficients

Term	Coef	SE Coef	T-Value	P-Value	VIF
Constant	42.50	1.61	26.39	0.000	
Temperature (°C)					
140	-12.25	2.79	-4.39	0.005	1.50
160	-2.00	2.79	-0.72	0.500	1.50
180	7.00	2.79	2.51	0.046	1.50

Time (min)					
20	-9.25	2.79	-3.32	0.016	1.50
30	-0.75	2.79	-0.27	0.797	1.50
40	2.25	2.79	0.81	0.451	1.50
Acid concentration(%)					
4	-13.00	2.79	-4.66	0.003	1.50
6	-3.25	2.79	-1.17	0.288	1.50
8	-0.25	2.79	-0.09	0.932	1.50

Regression Equation of the analysis is;

$$\begin{aligned}
 \text{Furfural yield (\%)} = & 42.50 \text{ Temperature (}^{\circ}\text{C)}_{140} - 2.00 \text{ Temperature (}^{\circ}\text{C)}_{160} \\
 & + 7.00 \text{ Temperature (}^{\circ}\text{C)}_{180} + 7.25 \text{ Temperature (}^{\circ}\text{C)}_{200} \\
 & - 9.25 \text{ Time (min)}_{20} - 0.75 \text{ Time (min)}_{30} + 2.25 \text{ Time (min)}_{40} \\
 & + 7.75 \text{ Time (min)}_{50} - 13.00 \text{ Acid concentration(\%)}_4 \\
 & - 3.25 \text{ Acid concentration(\%)}_6 - 0.25 \text{ Acid concentration(\%)}_8 \\
 & + 16.50 \text{ Acid concentration(\%)}_{10}
 \end{aligned}$$

APPENDIX II: FT-IR Spectrum of the Produced Furfural from Maize Cobs



Agilent Technologies

Sample ID:GM 3

Sample Scans:32

Background Scans:64

Resolution:4

System Status:Good

File Location:C:\Users\Public\Documents\Agilent\MicroLab\Results\GM 3_0000.a2r

Method

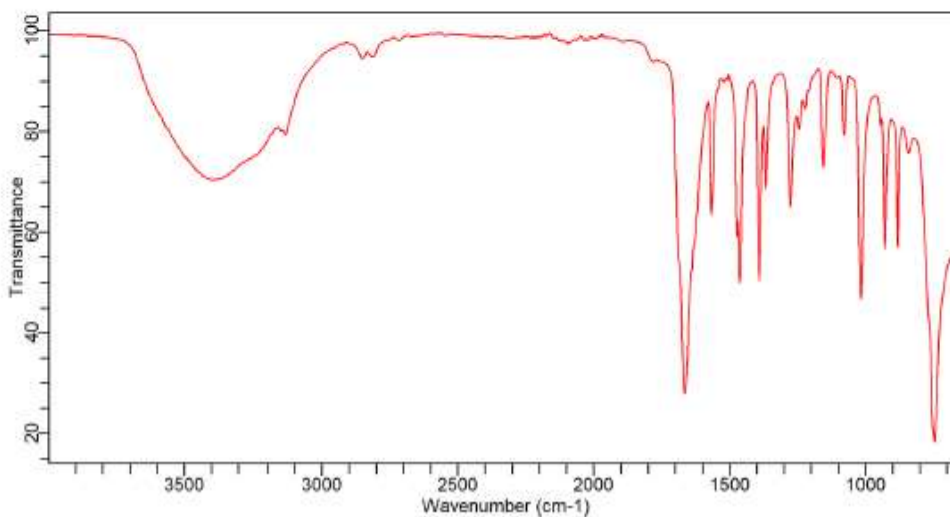
Name:C:\Users\Public\Documents\Agilent\MicroLab\Methods\Aminu 3.a2m

User:Central Lab

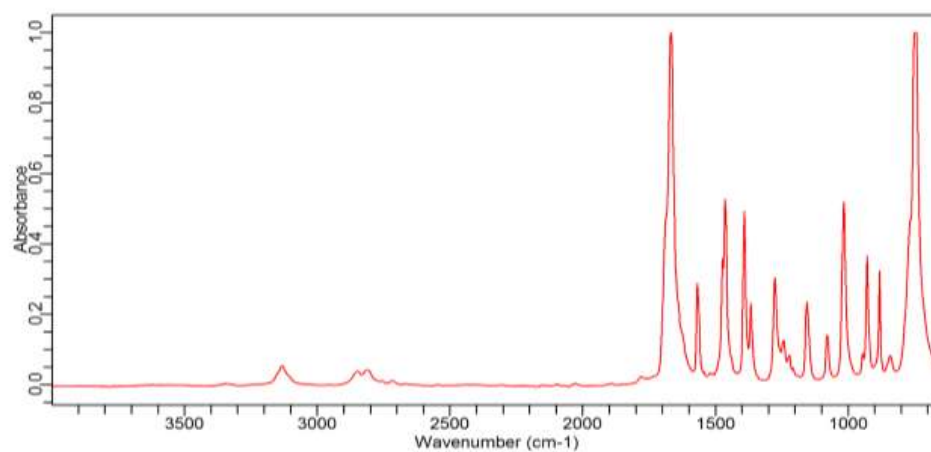
Date/Time:04/03/2019 4:00:09 PM

Range:4000 - 650

Apodization:Happ-Genzel



APPENDIX III: FT-IR Spectrum of furfural standard

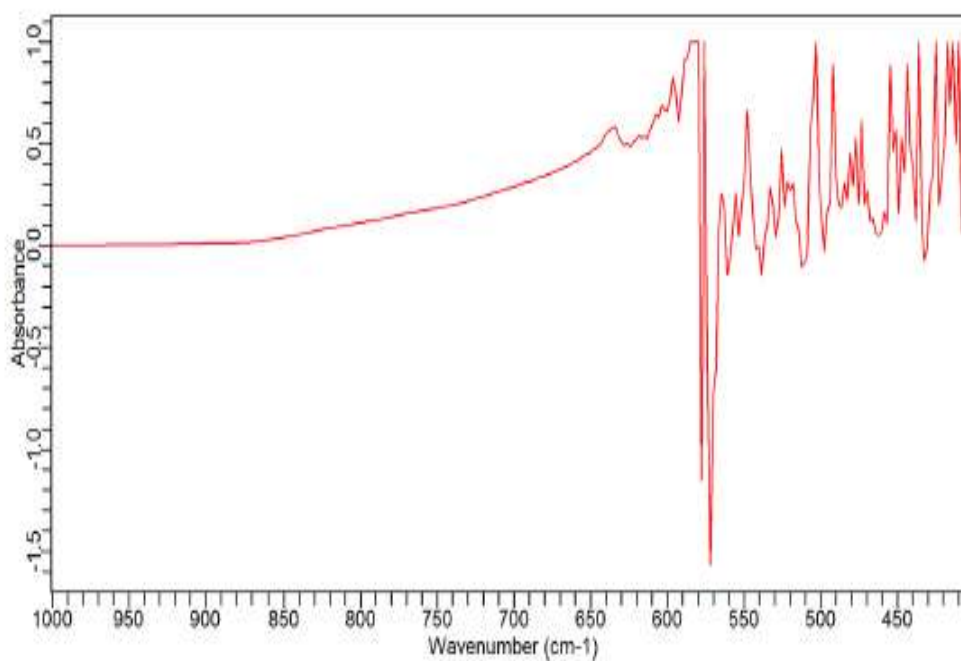


.a

Sample Scans:32
Background Scans:64
Resolution:4
System Status:Good

File Location:C:\Users\Public\Documents\Agilent\MicroLab\Results\GM 2_0000.a2r

User:Central Lab
Date/Time:04/03/2019 3:46:02 PM
Range:1000 - 400
Apodization:Happ-Genzel

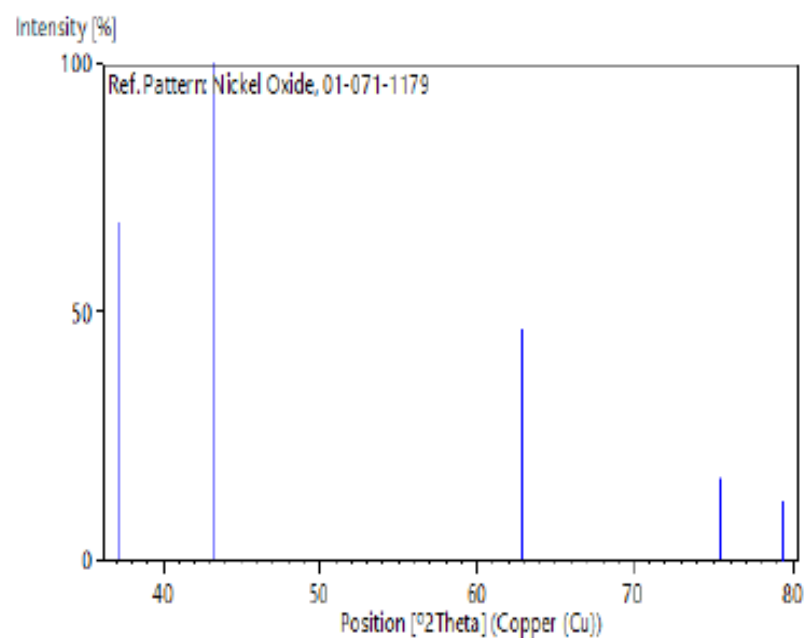


APPENDIX V: XRD Diffractogram of the Prepared NiOCatalyst

Peak list

No.	h	k	l	d [Å]	2Theta[deg]	I [%]
1	1	1	1	2.41217	37.246	68.0
2	2	0	0	2.08900	43.276	100.0
3	2	2	0	1.47715	62.863	46.5
4	3	1	1	1.25971	75.395	16.5
5	2	2	2	1.20608	79.387	11.8

Stick Pattern

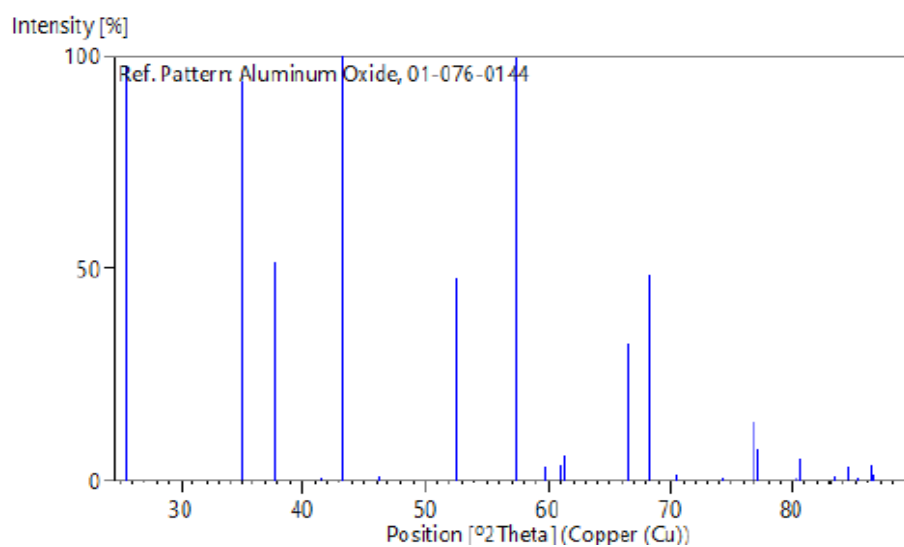


APPENDIX VI: XRD Crystallographic Parameters of the Prepared Al₂O₃ Catalyst

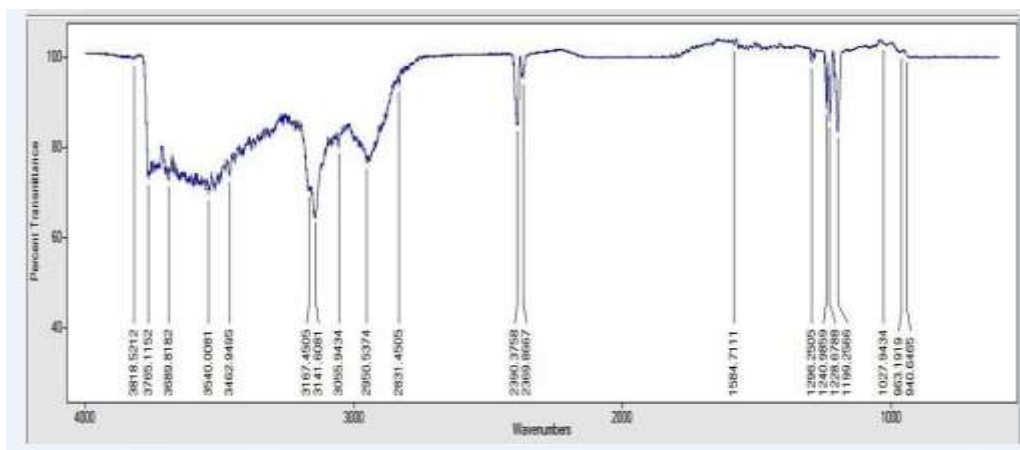
Peak list

No.	h	k	l	d [Å]	2Theta[deg]	I [%]
1	0	1	2	3.48042	25.574	97.4
2	1	0	4	2.55157	35.143	93.8
3	1	1	0	2.37949	37.777	51.5
4	0	0	6	2.16608	41.663	0.2
5	1	1	3	2.08559	43.350	100.0
6	2	0	2	1.96429	46.177	1.5
7	0	2	4	1.74021	52.546	47.5
8	1	1	6	1.60179	57.488	99.3
9	2	1	1	1.54667	59.741	3.5
10	1	2	2	1.51482	61.129	3.5
11	0	1	8	1.51138	61.283	6.2
12	2	1	4	1.40465	66.514	32.2
13	3	0	0	1.37380	68.209	48.5
14	1	2	5	1.33617	70.409	1.6
15	2	0	8	1.27578	74.283	0.4
16	1	0	10	1.23948	76.847	14.1
17	1	1	9	1.23451	77.214	7.6
18	2	1	7	1.19335	80.405	1.0
19	2	2	0	1.18974	80.700	5.3
20	0	3	6	1.16014	83.207	1.1
21	2	2	3	1.14726	84.354	3.4
22	1	3	1	1.13867	85.140	0.3
23	3	1	2	1.12578	86.351	3.6
24	1	2	8	1.12437	86.486	1.4
25	0	2	10	1.09928	88.971	5.2

Stick Pattern

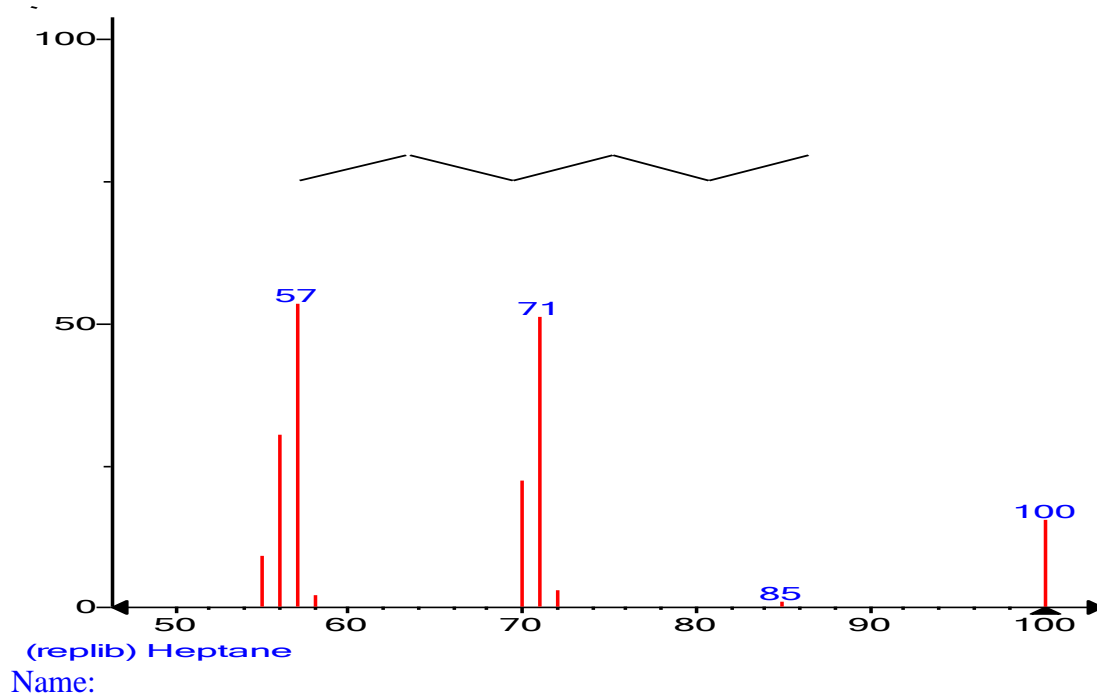
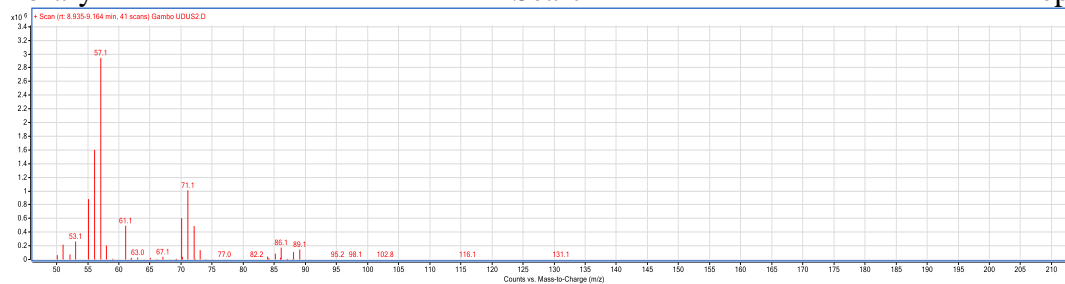


APPENDIX VII: FT-IR Spectrum of the Aldol Adducts



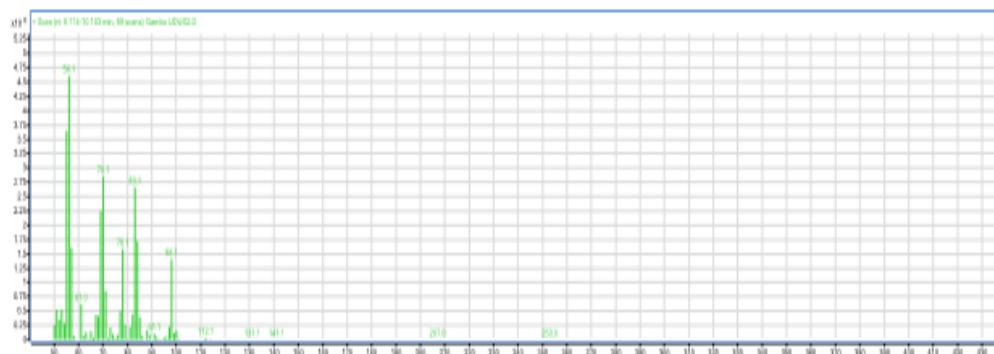
APPENDIXVIII: GC-MS Spectrum of the Hydrodeoxygenated Products

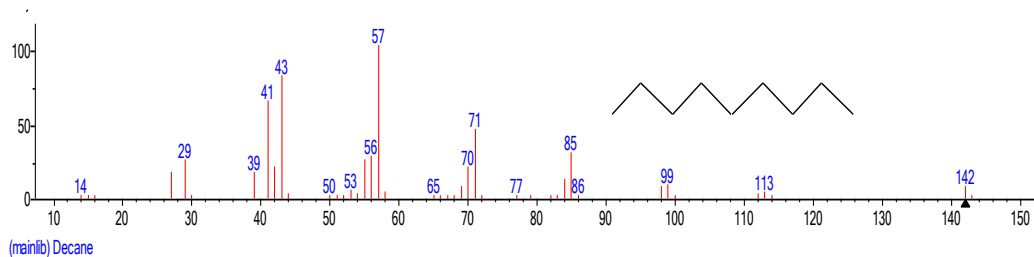
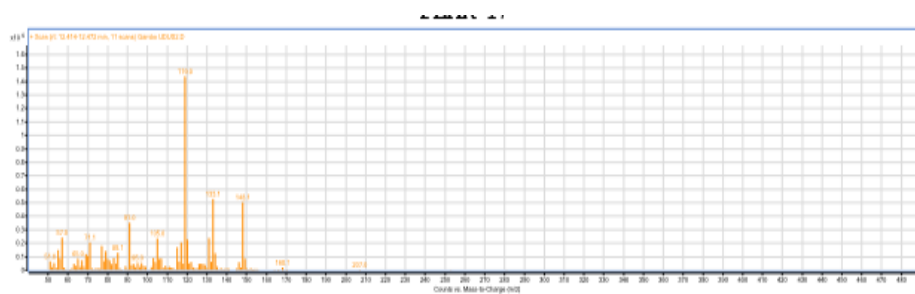
Library Search Report



Heptane
Formula: C_7H_{16}

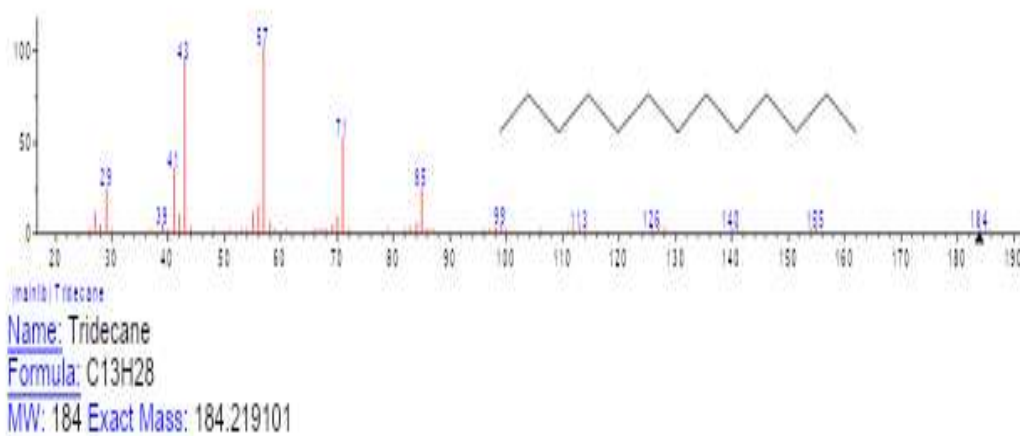
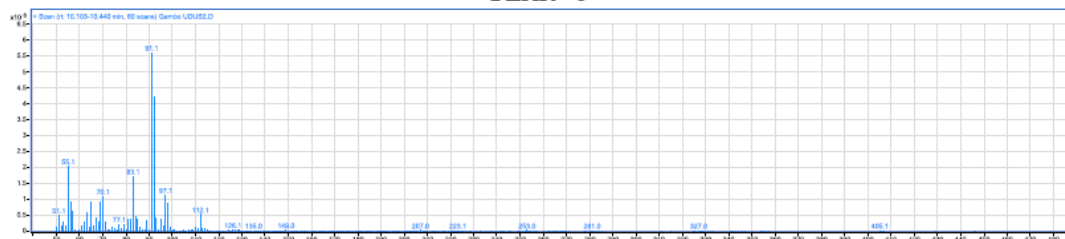
PEAK 5



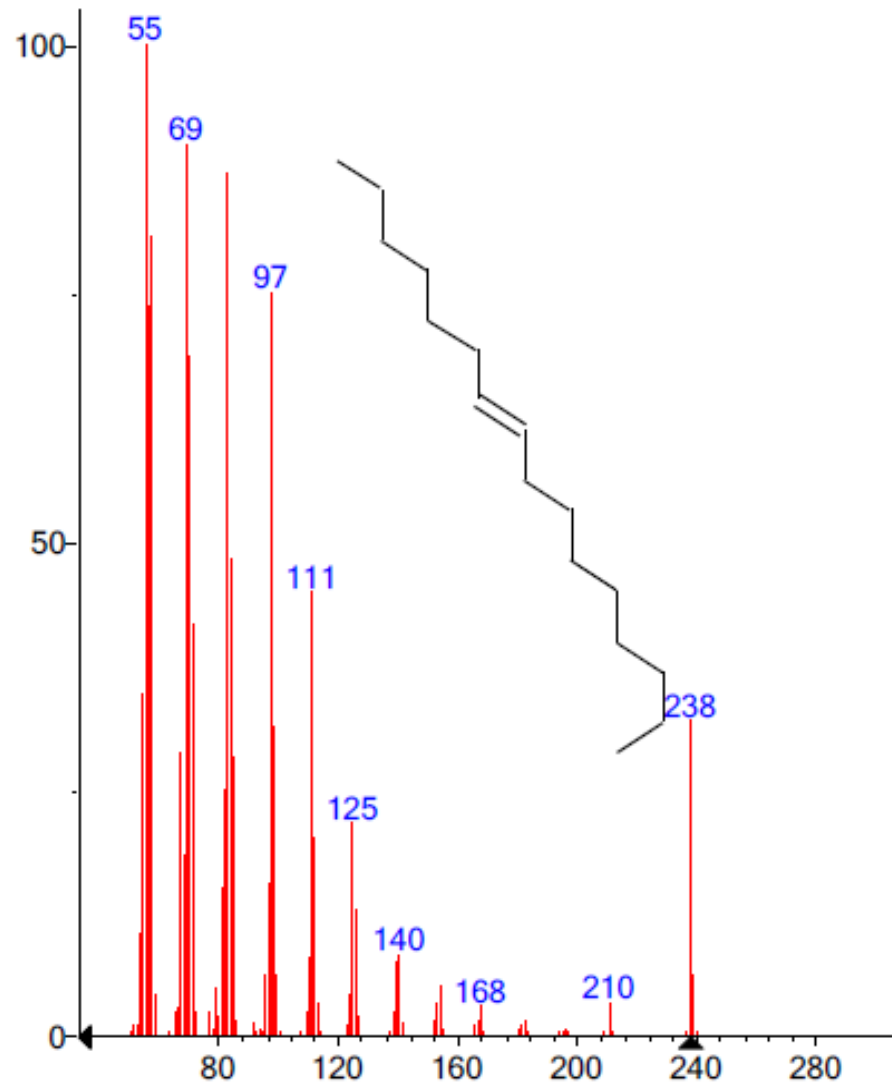
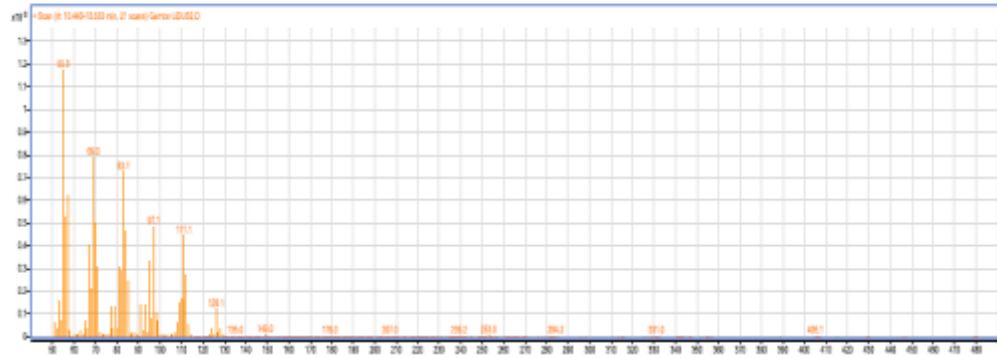


Name: Decane
 Formula: $C_{10}H_{22}$
 MW: 142 Exact Mass: 142.172151

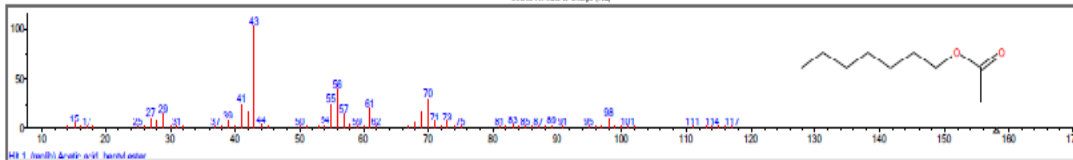
PEAK 6



PEAK 7

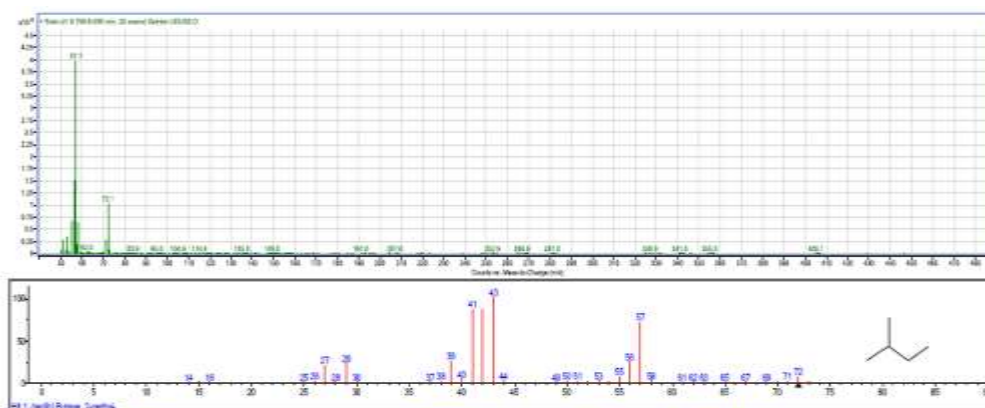


(replib) 8-Heptadecene

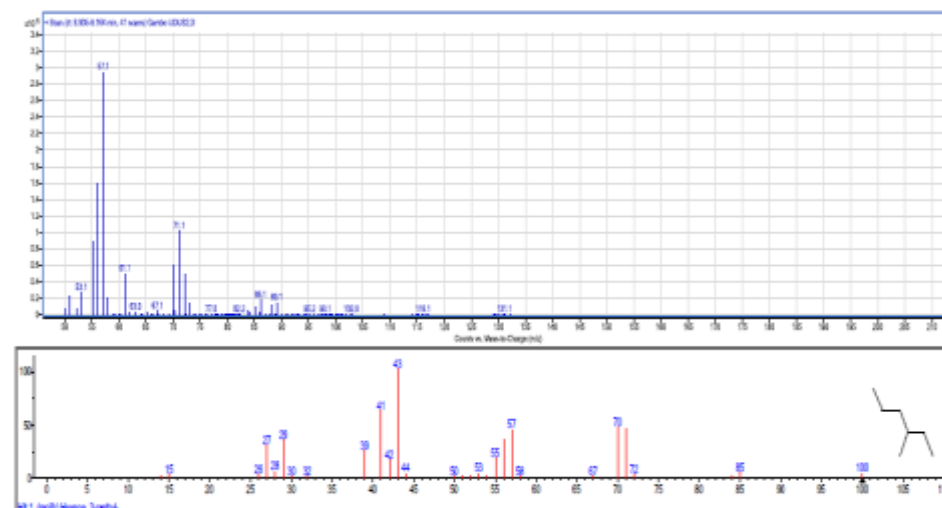


Formula: $C_9H_{18}O_2$

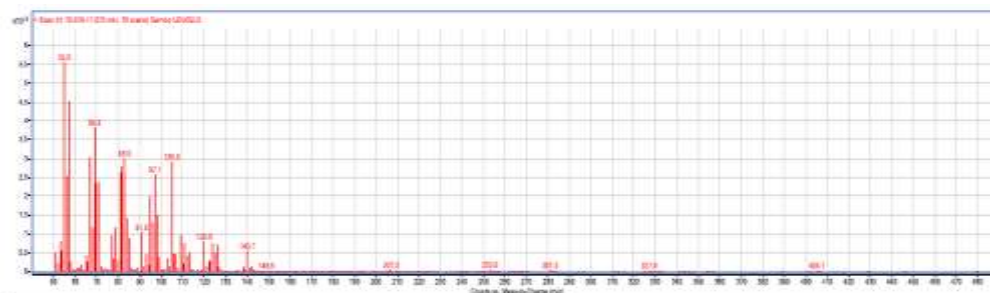
MW: 158 Exact Mass: 158.13068



Name: Butane, 2-methyl- Formula: C_5H_{12} MW: 72 Exact Mass: 72.0939



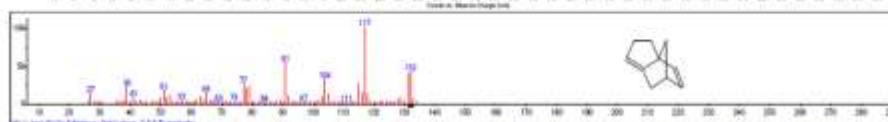
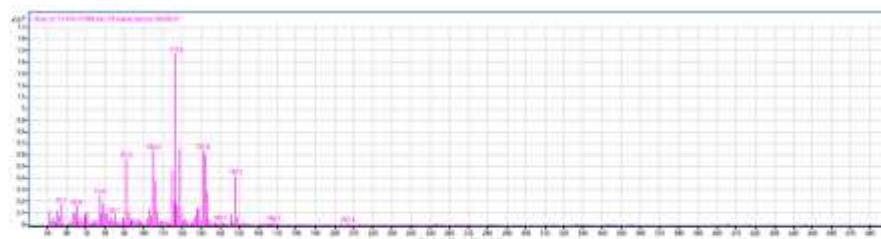
Name: Hexane, 3-methyl- Formula: C₇H₁₆ MW: 100 Exact Mass: 100.1252007



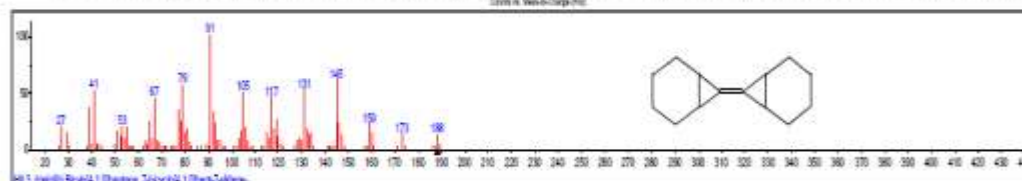
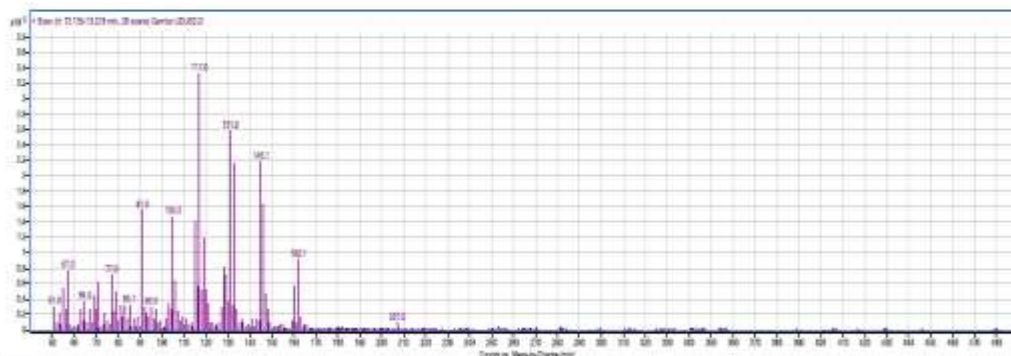
Name: trans-2-Dodecen-1-ol, trifluoroacetate

Formula: C₁₄H₂₃F₃O₂

MW: 280 Exact Mass: 280.165014



Name: 3a,6-Methano-3aH-indene, 2,3,6,7-tetrahydro- Formula: C₁₀H₁₂ MW: 132 Exact Mass: 132.093901



Name: Bicyclo[4.1.0]heptane, 7-bicyclo[4.1.0]hept-7-ylidene-

Formula: C₁₄H₂₀

MW: 188 Exact Mass: 188.156501